Chapter 8

Microwave Antennas for Energy Harvesting Applications

Dalia M.N. Elsheakh

Additional information is available at the end of the chapter

http://dx.doi.org/10.5772/64918

Abstract

In the last few years, the demand for power has increased; therefore, the need for alternate energy sources has become essential. Sources of fossil fuels are finite, are costly, and causes environmental hazard. Sustainable, environmentally benign energy can be derived from nuclear fission or captured from ambient sources. Large-scale ambient energy is widely available and large-scale technologies are being developed to efficiently capture it. At the other end of the scale, there are small amounts of wasted energy that could be useful if captured. There are various types of external energy sources such as solar, thermal, wind, and RF energy. Energy has been harvested for different purposes in the last few recent years. Energy harvesting from inexhaustible sources with no adverse environmental effect can provide unlimited energy for harvesting in a way of powering an embedded system from the environment. It could be RF energy harvesting by using antennas that can be held on the car glass or building, or in any places. The abundant RF energy is harvested from surrounding sources. This chapter focuses on RF energy harvesting in which the abundant RF energy from surrounding sources, such as nearby mobile phones, wireless LANs (WLANs), Wi-Fi, FM/AM radio signals, and broadcast television signals or DTV, is captured by a receiving antenna and rectified into a usable DC voltage. A practical approach for RF energy harvesting design and management of the harvested and available energy for wireless sensor networks is to improve the energy efficiency and large accepted antenna gain. The emerging self-powered systems challenge and dictate the direction of research in energy harvesting (EH). There are a lot of applications of energy harvesting such as wireless weather stations, car tire pressure monitors, implantable medical devices, traffic alert signs, and mars rover. A lot of researches are done to create several designs of rectenna (antenna and rectifier) that meet various objectives for use in RF energy harvesting, whatever opaque or transparent. However, most of the designed antennas are opaque and prevent the sunlight to pass through, so it is hard to put it on the car glass or window. Thus, there should be a design for transparent antenna that allows the sunlight to pass through. Among various antennas, microstrip patch antennas are widely used because they are low profile, are lightweight, and have planar structure.

Microstrip patch-structured rectennas are evaluated and compared with an emphasis on the various methods adopted to obtain a rectenna with harmonic rejection functionality, frequency, and polarization selectivity. Multiple frequency bands are tapped for energy harvesting, and this aspect of the implementation is one of the main focus points. The bands targeted for harvesting in this chapter will be those that are the most readily available to the general population. These include Wi-Fi hotspots, as well as cellular (900/850 MHz band), personal communications services (1800/1900 MHz band), and sources of 2.4 GHz and WiMAX (2.3/3.5 GHz) network transmitters. On the other hand, at high frequency, advances in nanotechnology have led to the development of semiconductor-based solar cells, nanoscale antennas for power harvesting applications, and integration of antennas into solar cells to design low-cost light-weight systems. The role of nanoantenna system is transforming thermal energy provided by the sun to electricity. Nanoantennas target the mid-infrared wavelengths where conventional photo voltaic cells are inefficient. However, the concept of using optical rectenna for harvesting solar energy was first introduced four decades ago. Recently, it has invited a surge of interest, with different laboratories around the world working on various aspects of the technology. The result is a technology that can be efficient and inexpensive, requiring only low-cost materials. Unlike conventional solar cells that harvest energy in visible light frequency range. Since the UV frequency range is much greater than visible light, we consider the quantum mechanical behavior of a driven particle in nanoscale antennas for power harvesting applications.

Keywords: energy harvesting (EH), antenna, rectenna, rectifier, nantenna, microstrip patch antenna (MPA), radio frequency (RF), wireless communications

1. Introduction of energy harvesting

Energy harvesting (EH) is defined as the process of extracting energy from the surroundings of a system and converting it into usable electrical energy, and it is more suitable for situations where the ambient energy sources are well characterized. EH could be an alternative energy supply technology. Such systems scavenge power from human activity, ambient heat, light, radio frequency (RF), vibrations, etc. Operated battery systems are used in various applications including wireless mobile phones and hand-held devices. However, increasing lifetime and durability of the battery are a matter of interest. Hence, recently energy harvesting from ambient to charge the battery or even to empower the system without any battery has gained momentum [1–4]. Processing power doubles every 2 years, battery capacity doubles every 10 years, however, we need a more efficient way to enable longer life. The ever increasing use of wireless devices, such as mobile phones, wireless computing, and remote sensing has resulted in an increased demand and reliance on the use of batteries. But the amount of energy available in the batteries is not only finite but also low, which limits the lifetime of the systems. It also has more advantages in systems with limited accessibility, such as those used in monitoring a machine or an instrument in a manufacturing plant used to organize a chemical process in a hazardous environment.

Harvesting ambient Wi-Fi transmission power through the rectenna can be a possible solution to extend the battery life of the active radio-frequency identification (RFID) tag. Global market

http://dx.doi.org/10.5772/64918

showed unprecedented growth in Wi-Fi hotspot deployments with an estimated 350% rise by 2015. Due to use of active RFID tags operating on very low power consumption, harvested Wi-Fi power in the submicrowatt range would not be deemed useless. The developed prototype was capable of delivering 20 μW of continuous power with an output voltage of 2 V at low excitation levels of 0.06g peak. Upper and lower Wi-Fi frequencies had the highest average power densities while the average power densities of 3G (2100 MHz) and LTE (2600 MHz) were the lowest. The highest peaks recorded were in the submicrowatt per square centimeter range for both Wi-Fi frequencies as well as the GSM/4G LTE 900 band, which were around 600–700 nW/cm^2.

Design of antennas with high gain and wide bandwidth is crucial to maximize the received power. Various antenna topologies have been reported in the literature for RF energy harvesting transparent or opaque antennas [5–7]. Maximum gain of 11.98 dB is reported in [6] but for a bandwidth of only about 20 MHz. Efficiency of the overall system greatly depends upon the matching between the rectifier and antenna. Variable input impedance of the rectifier with frequency and input power further limits total system efficiency. With semiconductor and other technologies continually striving toward lower operating powers, batteries could be replaced by alternative sources, such as DC power generators employing energy harvesting techniques. However, to introduce low power devices, the situation has changed with the technique being a viable alternative to batteries in different applications. Especially for wireless devices located in sensitive and difficult access environments where battery-operated equipment might not been previously possible. **Figure 1** shows some devices that potentially could be exploited for RF energy harvesting applications. These might be, but not limited to, TV and radio broadcasts, mobile phone base stations, mobile phones, wireless LAN, and radar. The transducer is typically an antenna or an antenna array—harvesting ambient electromagnetic energy. The recovered DC then, either powers a low-powered device directly or stored in a super capacitor for higher power low-duty-cycle operation. The block diagram of a basic energy harvesting system is shown in **Figure 2** [10].

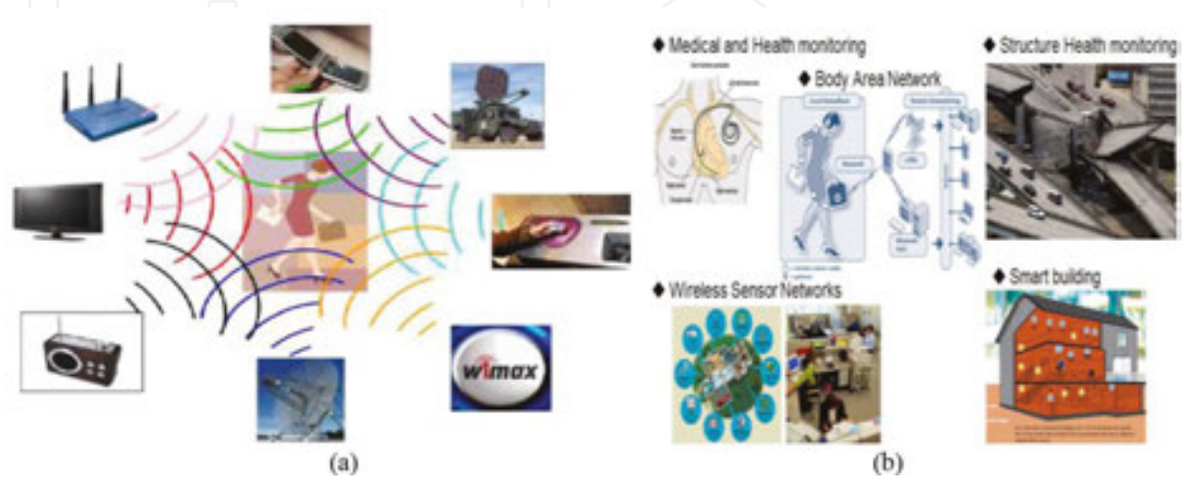

Figure 1. RF energy harvesting applications [8].

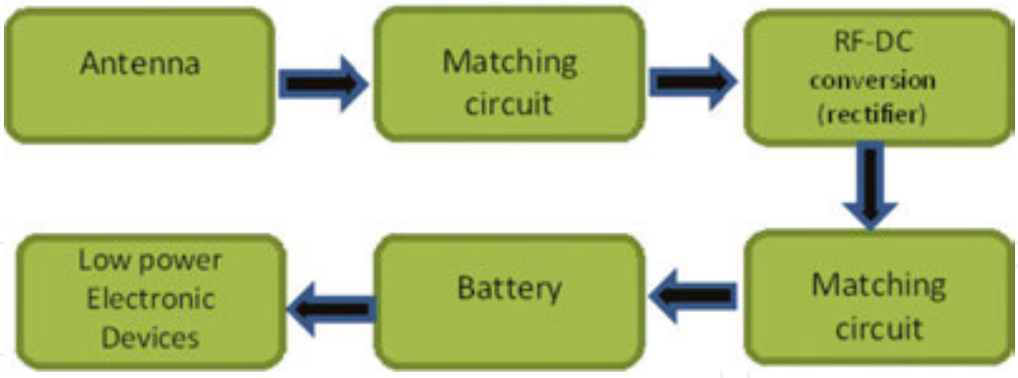

Figure 2. The block diagram of a basic energy RF harvesting system [9].

A nanoantenna (nantenna) is a nanoscopic rectifying antenna. It is an electromagnetic collector designed to absorb specific wavelengths that are proportional to the size of the nanoantenna. Nanoantennas may prove useful for converting solar radiation to electricity. Sufficient supplies of clean energy are intimately linked with global stability, economic prosperity, and quality of life. Finding energy sources to satisfy the world's growing demand is one of the society's challenges for the next half century. The world now uses energy at a rate of approximately 4.1 × 1020 J/yr, equivalent to continuous power consumption of 13 TW. The rapid technology development and economic growth worldwide are estimated to produce more than double the demand for energy to 30 TW by 2050 and more than triple the demand to 40 TW by the end of century. As a result of this, energy demands increased worldwide and as a consequence, the deleterious effects of hydrocarbon-based power such as global warming, air pollution, acid precipitation, ozone depletion, and forest destruction are increasingly apparent. The clean and renewable alternative energy resource is one of the most urgent challenges to the sustainable development of human civilization. About 120,000 TW of radiations from Sun reach Earth's surface far exceeding human needs [11–15].

2. Types of energy harvesting

The next few paragraphs provide an overview of some common energy harvesting schemes targeting devices in the list below. Solar energy, which involves converting the Sun's rays into useable electrical energy, is interesting but depends on the availability of daylight. The concept is certainly not foreign to the general population anymore. Solar-powered calculators and LED garden lights have been commonplaces for many years now. The efficiency of such conversion circuits has grown but the main detriment is the need for agreeable weather and timely use. Energy collection from natural sources at night is simply out of the question, limiting the user to daytime energy collection or requiring artificial sources of light with their own power supply needs. This method thus falls outside the scope of this work. Wind energy, for its part, requires bulky turbines for collection and necessitates the inclusion of mechanical components and brushings that are susceptible to wear and damage over time, if not properly maintained [11].

This is not an issue in traditional wind farm installations, where regular maintenance is expected to occur. The same expectation, however, cannot be placed on consumers and this energy source will thus not be further explored in this work. Kinetic energy harvesting aims to transform motional or inertial energy into a usable source of electrical charge via some type of transducer. In general, this requires some physical effort by the user, be it walking, running or otherwise shaking the device. Though this is not a problem for most able-bodied people, it could nonetheless be considered a hassle for a device intended for daily use, such as a personal cellular phone or a GPS unit. Radio-frequency energy, for its part, is readily available in all major industrialized centers and surrounding areas. Ambient energy harvesting, also known as energy scavenging or power harvesting, is the process where energy is obtained and converted from the environment and stored for use in electronics applications as shown in **Tables 1** and **2**. Usually this term is applied to energy harvesting for low power and small autonomous devices, such as wireless sensor networks, and portable electronic equipment. Some systems convert random motions including ocean waves into useful electrical energy that can be used by oceanographic monitoring wireless sensor nodes for autonomous surveillance. The literature shows that no single power source is sufficient for all applications, as energy sources must be considered according to the application characteristics [16–18] as shown in **Figure 3**, and **Figure 4** shows a diagram of a basic EH system.

Energy harvesting technique	Power density	Efficiency
Photovoltaic	Outdoors (direct Sun): 15 mW/cm^2 Outdoors (cloudiy): 0.15 mW/cm^2	Highest 32±1.5%
	Indoors: <10 μW/cm^2	Typical 25±1.5%
Thermoelectric	Human: 30 μW/cm^2/industrial: 1:10 mW/cm^2	±0.1% ±3.5%
Pyroelectric	8.64 μW/cm^2 at the temperature rate of 8.5°C/s	3.5%
Piezoelectric	250 μW/cm^2/330 μW/cm^2	
Electromagnetic	Human motion: 1–4 μW/cm^2	
Electrostatic	50–100 μW/cm^2	
RF	GSM900/1800 MHz: 0.1 μW/cm^2	50%
	Wi-Fi 2.4 GHz: 0.01 μW/cm^2	
Wind	380 μW/cm^2 at the speed of 5 m/s	5%
Acoustic noise	0.96 μW/cm^2 at 100 dB/0.003 μW/cm^2 at 75 dB	

Maximum power and efficiency are source dependent — excluding transmisssion efficiency.

Noise power densities are theoritical values.

Table 1. Power density and efficiency of energy harvesting techniques [11].

Energy source	Power density and performance
Acoustic noise	0.003 μW/cm²/0.96 μW/cm²
Temperature variation	10 μW/cm²
Ambient light	1 μW/cm²
Thermoelectric	30 μW/cm²
Vibration	200 μW/cm²
Vibration (piezoelectric)	300 μW/cm²
Air flow	50 μW/cm²
Push buttons	330 μW/cm²
Shoe inserts hand generators	30 W/kg
Heel strike	7 W/cm²

Table 2. Comparison of power density of energy harvesting methods [13].

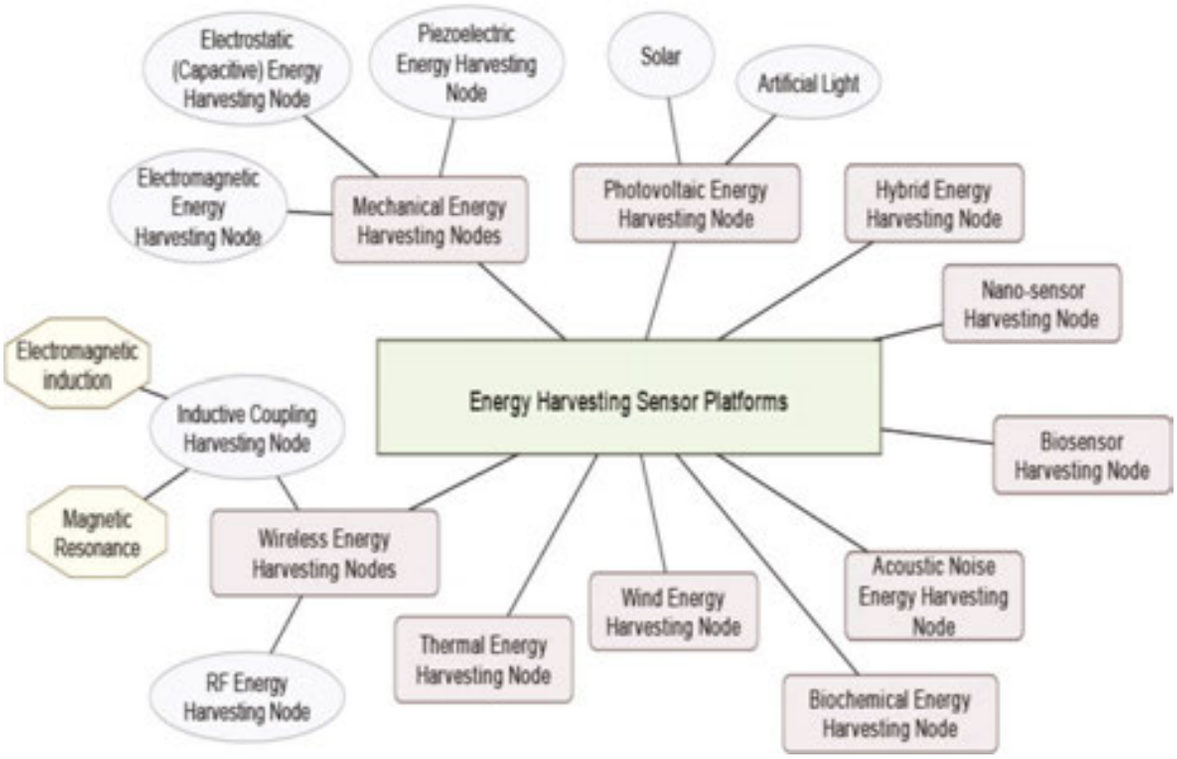

Figure 3. Different energy types (rectangles) and sources (ovals) [16].

http://dx.doi.org/10.5772/64918

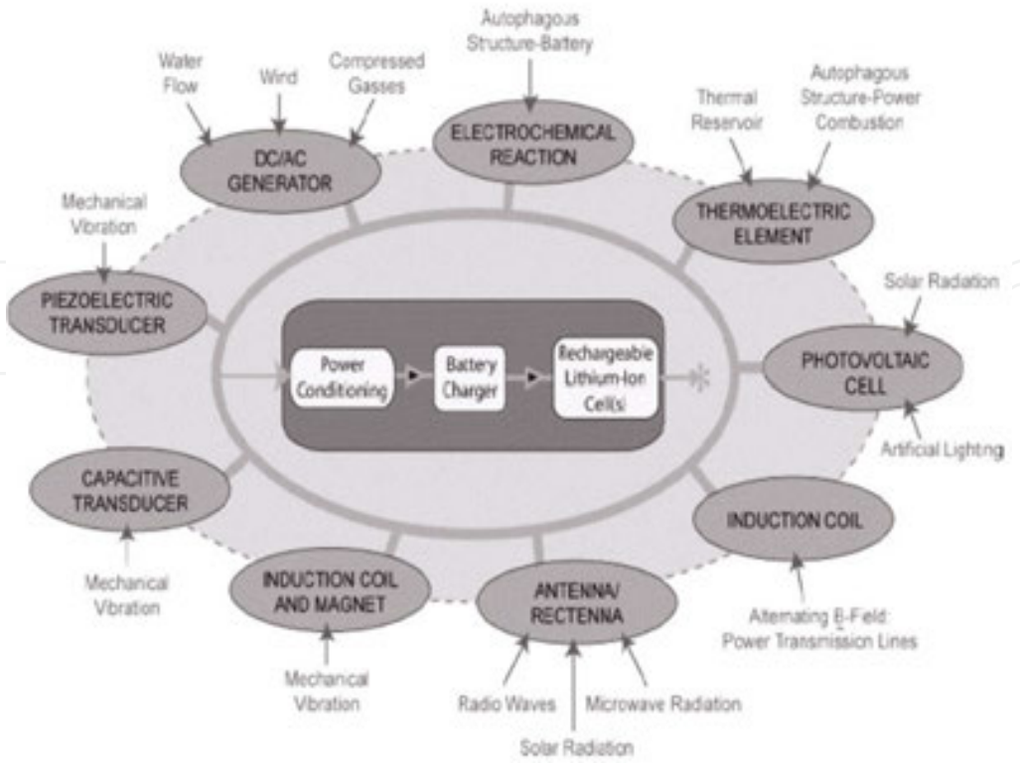

Figure 4. Example of the different radiating sources [19].

- Human body as mechanical and heat variations energy;
- Natural energy as wind, water flow or ocean waves, and solar energy;
- Mechanical energy as vibrations from machines from high-pressure motors, manufacturing machines, and waste rotations;
- Thermal energy as waste heat energy variations from heaters and friction sources;
- Light energy is divided into two categories of energy: indoor room light and outdoor sunlight energy. It can be captured via photo sensors, photo diodes, and solar photovoltaic panels;
- Electromagnetic energy as inductors, coils, and transformers is depending on how much energy is needed for the application. In addition, chemical, biological, and radiation can be considered ambient energy sources.

3. RF energy harvesting

The dramatic increase in demand for wireless devices has been met with a steady increase in infrastructure installations and thus an augmented source of radiated RF energy. This energy is in the air at virtually all times of the day and night, albeit at different power levels. A

study [2] of ambient global system for mobile communication (GSM) power in the Netherlands concluded that within a range of 25–100 m from a GSM base station, the summed average power present at all measured frequencies across the 935–960 MHz band varied between 0.1 and 3.0 mW/m^2 and depended greatly on the amount of GSM traffic at the time of measurement. This in itself poses a potential problem for energy harvesting devices: the small amount of energy available for harvesting is neither constant nor easily predictable. As such, one must ensure that any harvesting design remains useful over a wide dynamic range of available input power. Nonetheless, this form of ambient energy remains the most promising for use in consumer-oriented portable electronic devices, due to theoretical 24 h availability, lack of required physical effort to charge, and quasi-independence from weather conditions. Batteries have both effects as add extra size and add disposal to environmental pollution. A promising solution is available in capturing and storing the energy from external ambient sources for compact mobile and electronics devices; this technology is named as energy harvesting. Other names for this type of technology are power harvesting and free energy, which are derived from renewable energy [19]. Many research teams are working on reducing the consumption of the devices extending the battery life while the other teams have chosen to recycle ambient energy like in microelectromechanical systems (MEMS). The charging of mobile devices is easy because the user can do it but for other applications, the batteries remain a big problem as wireless sensor nodes that are located in difficult to access environments. This problem is due to the large number of devices and distribution in a wide area or located in inaccessible places. The rectification of microwave signals to DC power has been proposed for helicopter powering and solar power satellite [18–20].

DC power depends on the available RF power, the choice of antenna and frequency band, an energy harvesting technique using electromagnetic energy, specifically radio frequency. Communication devices generally have omnidirectional antennas that propagate RF energy in most directions to maximize connectivity for mobile applications [7]. The energy transmitted from the wireless sources for 10 GHz is much higher up to 30 W, however, only a small amount can be scavenged in the real environment. The rest of the power is dissipated as heat or absorbed by other materials. Radio-frequency identification (RFID) tags and implantable electronic devices are also used as RF power harvesting technique. This is because the wireless sensor nodes consume few μW in sleep mode and hundreds μW in active mode.

The electrical energy is then conditioned and used to charge a battery that stores and supplies the energy to a load, i.e., a WSN node. Each energy source has its own unique characteristics in terms of controllability, predictability, and magnitude; hence all these factors will need to be considered when choosing the most suitable source for a specific application. The number of consumer-oriented compact electronic devices (including, but not limited to, personal cellular phones, tablet PCs, and GPS units) has been growing at exponential rates for several years. Reliance on these devices for daily navigation, scheduling, and information-gathering activities has created an expectation of ever-longer battery life and less-frequent charging cycles with any new generation of product [21, 22].

This situation poses important questions to both the design engineers and the originating vendors of these devices. How can we power these circuits in a responsible manner? How can

engineers improve battery life and thus provide maximum "up" time for consumers? From the previous section, we are able to answer next question.

3.1. When does radio-frequency harvesting make sense?

Harvestable energy available can be installed and maintained in power devices that are difficult to reach. Harvestable energy is available for numerous devices, environmentally friendliness is required, and high uptime is demanded. Radio-frequency harvesting makes sense when used as remote patient monitoring, harmful agents detection, efficient office energy control, surveillance and security, detecting and tracking enemy troop movement, vineyard or other agricultural management, home automation, implantable sensors, long-range asset tracking and aircraft fatigue supervision.

The wireless devices are growing in many applications, such as mobile phones and sensor networks. Radio-frequency energy harvesting holds a promising future for generating a small amount of electrical power to drive partial circuits in wirelessly communicating electronics devices. As remote patient monitoring, harmful agents detection, efficient office energy control, surveillance and security, detecting and tracking enemy, troop movement, vineyard or other agricultural management, home automation, implantable sensors, long-range asset tracking, aircraft fatigue supervision, and reducing power consumption have become a major challenge in wireless sensor networks. As a vital factor affecting system cost and lifetime, energy consumption in wireless sensor networks is an emerging and active research area. RF energy is currently broadcasted from billions of radio transmitters around the world, including mobile telephones, hand-held radios, mobile base stations, and television/radio broadcast stations. **Figure 4** shows the huge amount of radio waves in air. From ambient sources enables the wireless charging of low power devices and has other benefits associated with product design, usability, and reliability. Battery-free devices can be designed to operate upon demand or when sufficient charge is accumulated. However, while many researchers have made an effort to increase the receiving RF power, the RF energy accumulated from air space is very limited, less than 1 W. However, several experiments were conducted using highly efficient receivers that were capable of receiving digital TV signals in the range of 40–20 dBm as in [23]. The system composed of a rectenna, which is a particular type of antenna that rectifies incoming electromagnetic waves into DC current. A typical rectenna consists of four main components: antenna, prerectification filter, rectifying circuit, and DC pass filter. A microwave antenna collects incoming RF power as shown in **Figure 5(a)**. An input low-pass filter (LPF; prerectification filter) suppresses the unwanted higher harmonics rejected by the rectifying circuit and also provides matching between the antenna and the rectifier [24]. A traditional rectenna system composed of a dipole element or a mesh of dipoles that capture microwave energy and Schottky diode for the rectification process. Different types of rectenna elements have been proposed recently. The antenna could be, for example, dipole, Yagi-Uda, microstrip, monopole, loop, coplanar patch, spiral, or even parabolic [25], whatever opaque or transparent antenna, as shown in **Figure 5(b)**. A half-wave parallel rectifier is used as a voltage doubler structure to theoretically double the output DC voltage or a dual-diode full-wave rectifier to increase the conversion efficiency [26].

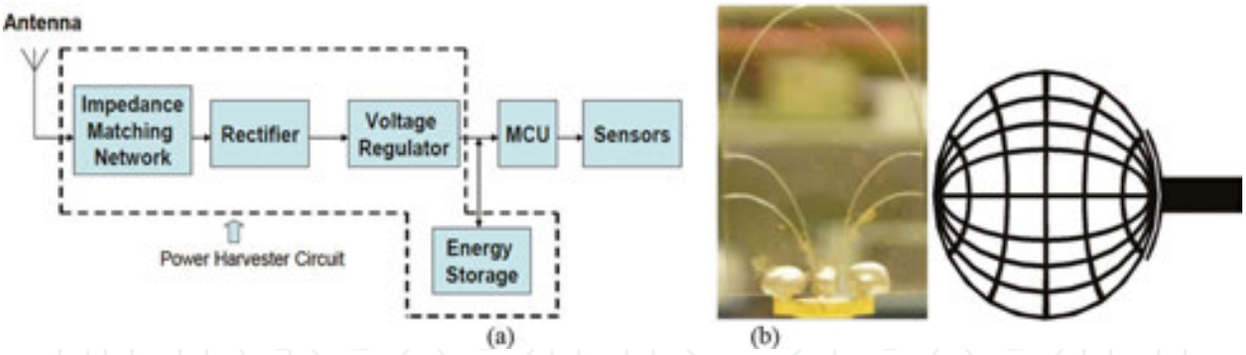

Figure 5. (a) Diagram of a typical power harvesting circuit and (b) different antenna shapes used.

4. Types of RF energy harvesting (EH)

RF signals used for wireless communication systems will be the most suitable energy source because heat, light, and vibration are not always available at every place. Electromagnetic energy exists in the form of alternating magnetic fields surrounding AC power lines or radio waves emitted by nearby transmitters. There are two types of EH application devices: near field and far field.

4.1. Far-field devices

The wearable rectenna well suited for energy harvesting for ultrahigh frequency (UHF) band and a tetra-band genetic-based rectenna designed to harvest from the global system for mobile communications, the Universal Mobile Telecommunications System (UMTS), and Wi-Fi RF sources [27].

4.2. Near-field devices

In this section, two examples of devices operating in the near-field region of the source are reported. The first one is a harvester optimized for power generation from spurious emissions of compact fluorescent lamps (CFLs). The second example of application is a near-field link optimized for powering IMDs. In both cases, a wireless power transfer is implemented by inductive coupling [28].

Choosing the frequency is an important consideration in RF energy harvesting systems and at the same time might be environment specific. Wavelengths up into the low GHz for indoor application would be a better choice, due to their ability to propagate well in these environments, rather than lower VHF/UHF transmissions for outdoor or remote location harvesting applications. Generally, in the modern built environment, GSM mobile phone signals are prevalent and propagate well both into and out of buildings, offering harvesting potential from both the GSM base stations and the user's handsets. This is a promising EH environment because of the tremendous growth of mobile phone usage in Egypt, one of the best growing countries with more than 97 million subscribers [29] (**Table 3**).

Energy source	Classification energy	Power density	Weakness	Strength
Solar power	Radiant	100 mW/cm^3	Require exposure to light, and low efficiency if device is in building	Can use without limit
RF waves	Radiant	0.02 μW/cm^2 at 5 km from AM radio	Low efficiency inside a building	Can use without limit
RF energy	Radiant	40 μW/cm^2 at 10 m	Low efficiency if out of line of sight	Can use without limit
Body heat	Thermal	60 μW/cm^2 at 5°C	Available only when temperature difference is high	Easy to build using thermocouple
External heat	Thermal	135 μW/cm^2 at 10°C	Available only when temperature difference is high	Easy to build using thermocouple
Motion body	Mechanical	800 μW/cm^3	Motion	High power density, not limited on interior and exterior
Flow blood	Mechanical	0.93 W at 100 mm	Low conversion efficiency	High power density, not limited on interior and exterior
Flow air	Mechanical	177 μW/cm^3	Low conversion efficiency inside a building	High power density
Vibrations	Mechanical	4 μW/cm^3	Has to exist at surrounding	HPD, not limited on interior and exterior
Piezoelectric	Mechanical	50 μW/cm^2	Has to exist at surrounding	HPD, not limited on interior and exterior

Table 3. Comparison of energy harvesting sources for WSNs [29].

5. Radio-frequency energy harvesting system description

During the daytime, various electronic devices are used, and hence, ambient RF energy in their bands is expected to be time dependent, with more energy available during the daytime than at nighttime. So in order to be able to make fair comparisons between locations, measurements were taken over the day on weekdays over a period of 1 month. Electric field strength was measured between 0.3 and 2.5 GHz/WLAN using an Agilent/Rohde & Schwarz, Field Fox RF analyzer with different types of antennas. It is important to note that the spectral measurements were undertaken during the analog-to-digital switches. Therefore, the measurements for wireless communications may represent an underestimate of present RF power levels when measured now. The effective isotropic-radiated power (EIRP) in different countries, which could be collected in the wireless frequency band, is shown in **Table 4** [30].

Country	Frequency band (MHz)	Power (EIRP)
The United States	902–928	4 W
The United Kingdom	865.6–867.6	2W ERP/3.28 W EIRP
Japan	952–954	4 W

Table 4. Frequency allocation and permitted radiated power for the selected UHF [30].

In order to achieve maximal energy collection by targeting several highly used frequency bands, a multifrequency antenna design with an omnidirectional radiation pattern will be targeted. Although a circular polarization would be ideal, it will not be used in this case, due the added implementation space required and tight design sizing constraints. **Table 5** [31] aims to compare the aforementioned antenna topologies. Here, the physical size is described in relation to wavelength; multiband behavior indicates the ability of the topology to cover more than one operational band at a time; and bandwidth describes the frequency range covered around the central operating frequency. Qualitative descriptions are also for the theoretical radiation pattern, the difficulty level of fabrication, the ability to quickly scale the design for new operating frequencies, and the level of difficulty relating to properly feeding/tapping the antenna.

Energy source harvesting power	Harvesting power	Energy source harvesting power	Harvesting power
Vibration/motion		RF/EM	
Human	4 μW/cm^2	GSM	0.1 μW/cm^2
Industry	100 μW/cm^2	Wi-Fi	0.001 mW/cm^2
Temperature difference		Solar	
Industry	1–10 mW/cm^2	Outdoor	10 mW/cm^2
Light		Indoor	<0.1 mW/cm^2
Indoor	10 μW/cm^2	Acoustic	
Outdoor	10 mW/cm^2	75–10 dB of noise	0.003–0.96 μW/cm^2
Human power source		Human power source	
Body heat	0.2–0.32 W (neck)	Walking	5–8.3 W

Table 5. Energy harvesting estimates [31].

5.1. Rectenna design

The approach of many papers (including [32]) has also explored the joint design of antenna and rectifier as one complete entity, commonly referred to as a "rectenna." This integrated design method aims to reduce the size of the final design, as well as streamline the design process, by eliminating unnecessary intermediate steps. For example, [33] shows the use of a source pull simulation on the rectifying diode, utilizing harmonic balance to determine the optimal source impedance that the antenna should present to the diode over a range of

expected input power levels. These results will allow the antenna designer to use this as a design goal while designing the antenna, eliminating the need for a separate matching network [34].

5.2. Input matching and detector

To assure maximum power delivery for good antenna, the impedance-matching network performs impedance transformation. **Figure 6** illustrates the impedance transformer role, where Vin and Zin are the induced voltage and the input impedance of the impedance transformer, respectively, and the YIC and VIC are the input admittance and input voltage of the rectifier, the transformer impedance is composed of reactive lossless components. When $V_{IC} = \left(\frac{\sqrt{Re(\{Yin}}{\sqrt{Re(\{Yic}}/2\right)V_{in,}$ the impedances are nearly matched and it turns out the impedance transformer to also work as a voltage booster [35]. When L-type matching network is used, the relationship of the input and output conductances can be derived as $Re(\{Yin = (1 + Q^2 Re(Y_{ic}))$, where Q is the quality factor of the matching network at resonate frequency. For a lossless L-type matching network consisted of L and C, Q = ω0 C/ Re{Yic}, where ω0 is the resonate frequency, as a result $= \sqrt{1 + \frac{Q^2}{2}}V_{in}$. A high Q is required in order to achieve a high voltage gain [36].

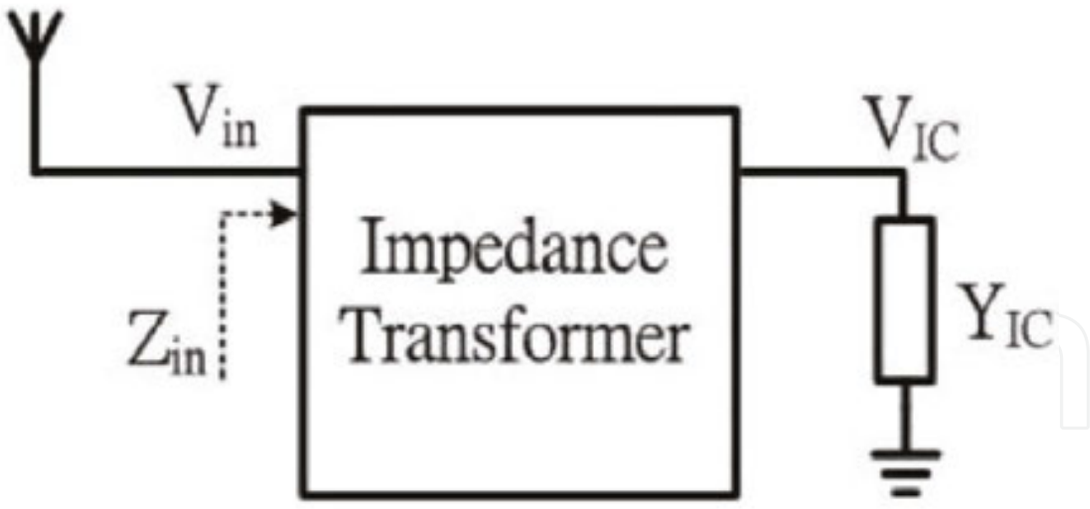

Figure 6. Impedance transfer.

5.3. Power combining

Power combining has been demonstrated in several ways in the literature, including RF combining of the received power from multiple antennas. The end goal is always to increase the amount of harvested RF energy. The author of [37] demonstrated a different configuration

by grouping antennas tuned to a handful of targeted frequencies, though not in an energy harvesting application. The configuration combined Koch fractal loops at 915 MHz with meandered structures aimed at the 2.45 GHz band (see **Figure 7**). It is shown that combining at the RF level allows more optimum power harvesting near the main receiving lobe, when speaking of directional antennas. Nonetheless, once the angle of reception is deviated more than ±25° from the main lobe, the DC combination proves to offer slightly superior performance.

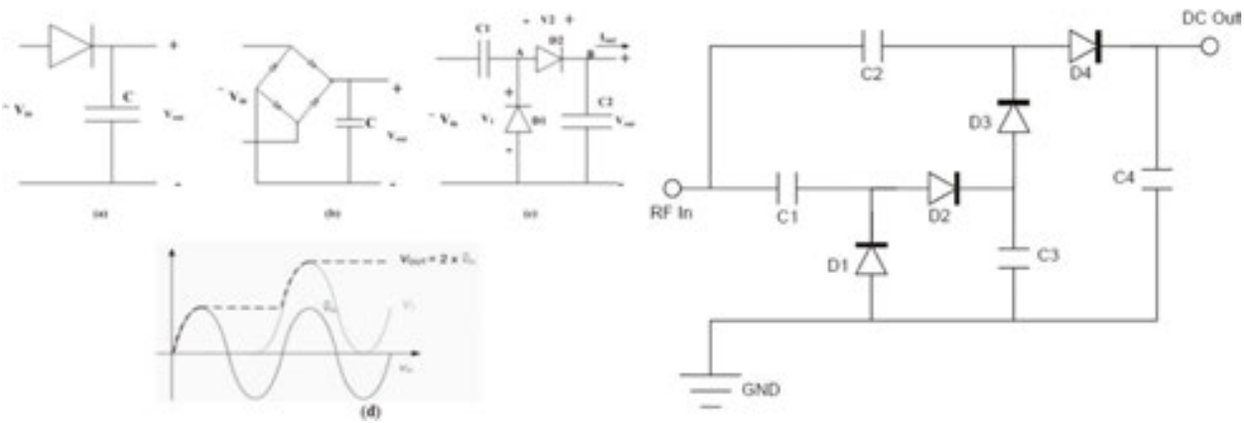

Figure 7. (a) Diode, (b) bridge of diodes, (c) a voltage multiplier rectifier, (d) its waveforms during the transient, and (d) three bridges of voltage multiplier.

5.4. Impedance matching

Impedance matching is another challenging concern, which stems primarily from the inconsistent impedance of the nonlinear rectifying elements (whether considering diodes or transistors). As varying potential is applied to the junction, junction capacitance changes slightly. Thus, the impedance varies with the amount of input power presented to it. Consequently, any static matching network is only truly effective over a finite input power range. This problem is clearly magnified when there are multiple antennas and/or multiple rectifiers. An increase of 100–150% in rectifier efficiency was noted through simulation [38, 39].

5.5. Rectification

Rectifier circuits provide a DC output voltage at the load. There are three main options for the rectifier. **Figure 9** shows that the bridge diode provides an output DC voltage to the load (VOUT) whose amplitude is lower than that of the incoming signal. The voltage rectifier is a multiplier, so it multiples the peak amplitude of the incoming signal. Due to long distances, the DC voltage level is not high enough to power an electronic circuit, so the voltage rectifier multiplier is used. Several attempts to enhance the efficiency of diode rectification have also been made in the literature. The use of PMOS transistors to replace diode-connected NMOS transistors as rectifying elements allows a reduction in threshold voltage and a 5% relative

increase in rectifier efficiency [41]. This is an interesting option for CMOS implementations (but outside the scope of this work). The idea of resistor emulation for the purpose of tracking the peak power point over a wide range of incident power levels is explored in [42]. This effectively increases the optimal input power range over which the rectifier remains efficient. Since the implementation at hand does not enjoy the luxury of predetermined input power levels, several papers have also proposed the notion of sacrificial biasing, a technique where DC bias is applied to the rectifying element's input in order to reduce the required threshold voltage needed to allow conduction. At the expense of some output current, the circuit's efficiency was shown to increase by 60% over the nonsacrificial equivalent NMOS circuit [43].

5.6. Energy storage

Most common energy storage device that used in a sensor node is a battery, either nonrechargeable or rechargeable. For example, a nonrechargeable battery (alkaline) is suitable for a microsensor with very low power consumption (50 μW). Other example, a rechargeable battery (lithium ion) is used widely in sensor nodes with energy harvesting technology. Various factors affect the quality of these batteries but the main factors are cost and price. Batteries are specified by a rated current capacity C, expressed in ampere-hour. It describes the rate at which a battery discharges without significantly affecting the prescribed supply voltage potential difference. However, the discharge rate increases when the rated capacity decreases [44, 45]. This means that a 1000 mAh battery produces 1000 mA for 1 h, if it is discharged at a rate of 1 C. 1 C is often referred to as a 1 h discharge. Likewise, a 0.5 C would be a 2 h and a 0.1 C, a 10 h discharge.

$$T = \frac{C}{I^n} \tag{1}$$

where C is the battery capacitance expressed in ampere-hours, I is the drawn current in ampere (A), T is the time of discharge in seconds, and n is the Peukert number, a constant that directly relates to the internal resistance of the battery. The Peukert number indicates how well a battery performs under continuous heavy current [45].

6. Antenna design used in RF energy harvesting

The antenna innovations in the aforementioned works involve explorations of new antenna variations, including, but not limited to, rectangular antennas and arrays thereof, slotted patch antennas, gap-coupled microstrip antennas, circular patch antennas, folded dipoles, circularly polarized spiral antennas, planar inverted-F antennas (PIFA), and fractal (particularly Koch) monopole, dipole and patch antennas. From the previous information, the antenna needs to offer [46]:

- Narrow band/multiband operation.

- CP polarization.
- Matching impedance for maximum power transfer to the following rectifier circuitry.

Antenna with different shapes and types has been employed in RFEH applications, from the simple dipole to more complex designs such as the bow tie or spiral antenna. It gives good performance in terms of polarization; however, it is generally limited to broadband designs with a few hundred MHz bandwidths. Multi narrow-band frequency designs are usually limited due to the need for a complex feed arrangement to each antenna element. Now there are many designs in [47], which provide three bands that based on close-coupled resonant elements [47].

CP has become one of the essential characteristics in designing rectennas [48]. CP prevents the variation of the output voltage due to the rotation of the transmitter or receiver. Dipoles or patch antennas are used in conventional rectenna design. The coplanar strip line is used to feed the dipole antennas. It can be used to combine several antenna elements for higher gain and also to form an antenna array more easily. Many CPS-fed rectennas have been recently in [49] and by using a high-gain antenna, reduces the number of rectenna elements needed. In most cases, an antenna with a higher gain will cover a larger effective area. So, there is a tradeoff between the antenna gain and the antenna area. However, even with circular polarization, the efficient power transmission still requires a precise main beam alignment between the transmitter antenna and the receiver rectenna array. The transmitter antenna usually has a quite narrow beam width at the broadside.

Despite the fact that a circularly polarized antenna can maintain a constant output voltage when the transmitter or the receiver rotates, it cannot prevent the output voltage variations due to improper main beam alignment. The array aperture of the nonuniform array can be designed to form a uniform amplitude antenna pattern on both the E-plane and H-plane and also widen the main-lobe beam width. The broadened main beam width rectenna keeps the output voltage invariant even if the rectenna has an improper beam alignment. This method indeed makes the main beam broadened, numerous antenna elements with various sizes are needed and the nonuniform array gain may be lower than that of the uniform array.

6.1. Opaque antenna

The rapid development of microstrip antenna technology began in the late 1970s. By the early 1980s, basic microstrip antenna elements and arrays were fairly well established in terms of design and modeling. The microstrip patch antenna (MPA) is recently used as a low-profile, flush-mounted antennas on rockets and missiles showed that this was a practical concept for use in many antenna system problems [49]. Different shapes of antennas were developed and their applications were extended to many other fields. A major contributing advance of MPA is the revolution in electronic circuit miniaturization brought about by developments in large-scale integration. Traditional MPA antennas are often bulky and costly part of an electronic system, and MPAs based on photolithographic technology are seen as an engineering break-through. The MPA structure consists of a radiating patch on one side of a dielectric substrate with a ground plane on the other side. The patch is generally made of a conducting material

such as copper or gold and can take any possible shape, such as square, rectangular, thin strip dipole, circular, elliptical, or triangular. Square, rectangular, dipole, and circular shapes are the most common because of ease of analysis and fabrication, and their attractive radiation characteristics, especially low cross-polarization radiation [50].

Several feed MPA configurations are used while the most popular ones are the microstrip line, coaxial probe, aperture coupling, and proximity coupling [51].

6.2. Compact and multiband microstrip antennas

Different other microstrip structures are successful candidates as microstrip planar inverted F-antenna with different geometrical radiator shapes. The main goal is to design antennas for wireless communication applications where the space value of the antenna is quite limited while it reserves the characteristics of multiband, lightweight, low cost, robustness, diversity, packaging capabilities and ability for RF PIN switches/MEMS integration for smart antenna systems. Several researches in literature concentrate on these antenna types and their developments. Famous techniques for antenna size reduction include dielectric loading to reduce the electrical size, top hat loading, and use of shorting PINs or plates [52]. Dielectric loading usually accompanied by bandwidth reduction and cost increase, so it is not a likely approach. The interesting choices are slot-coupled multiresonators, printed spiral antennas, planar inverted "F" antennas (PIFA), and a fractal implementation, such as the Koch. When simplicity of fabrication is considered, the PIFA and spiral antenna designs are more dependent on manufacturing tolerances [53, 54].

6.3. Transparent antenna

Transparent antenna was first presented by the National Aeronautics and Space Agency (NASA) when researchers Simmons and Lee demonstrated the use of AgHT-8 to produce single patch antennas to operate at 2.3 and 9.5 GHz. To design and produce workable antennas, different materials are used such as indium tin oxide (ITO) and aluminium-doped zinc oxide. Except for those produced using ITO or AgHT, most of the so-called transparent antennas are simply antennas constructed by coating transparent polymer substrates with nontransparent conductive traces of silver or other conductive ink [40, 55]. Some selected shapes of the transparent antennas as shown in **Figures 8** and **9** cannot be really categorized as fully transparent antennas since the traces are visible to the eye. The transparent antennas in this section are those that are fully transparent, in other words, even the conductive traces are transparent and discreet to the eye.

The main function of a transparent rectenna is to convert RF energy to DC power, the main design challenge is to obtain resonable conversion efficiency, and there are basically two methods to achieve this goal: First, transparent antennas being built on materials that are discreet, flexible, conformal, conductive, and having the ability to provide good antenna performance on glass to serve as the "last mile" link in subsequent generation communications after 4G have been the basis for this contention. Second, using transparent conductive oxide polymer (TCO), AgHT and its properties, and culminates in the development of a transparent

antenna that can be integrated with photovoltaic for window glass applications on homes and buildings. There are different applications such as on-body wireless communications in health care monitoring were also analyzed and presented [56, 57].

Figure 8. Transparent radiator of the monopole antenna.

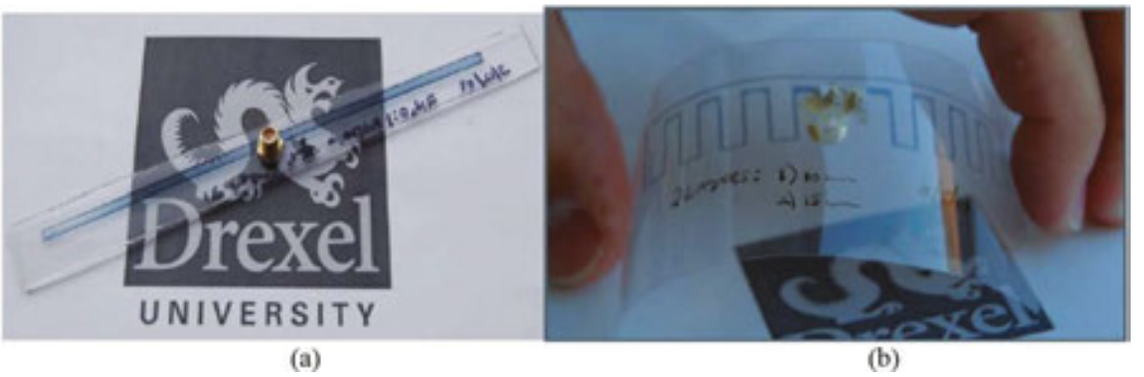

Figure 9. (a) RFID 1/2 dipole antenna and (b) RFID meandering dipole antenna [40].

Transparent conductive oxides have a variety of uses as shown in **Figure 10**; one common use is its ability to reflect thermal infrared heat. This characteristic is exploited to make energy-conserving windows. An example of which is AgHT, which is effectively a sun-shielding film manufactured by Solutia Inc. This low-emissivity window application is currently the largest area of use for TCOs. It is to collect the reasonable power and deliver it to the rectifying diode, and the second one is to suppress the harmonics generated by the diode that reradiate from the antenna as the power lost. For increasing the conversion efficiency by using several broadband antennas, large antenna arrays and circularly polarized antennas have been designed. This antenna receives relatively reasonable RF power from various sources, and antenna array increases incident power delivered to the diode for rectification. Antenna array is an effective means of increasing the receiving power but a tradeoff arises between the antenna size and the radiation gain. To increase the efficiency by second method, LPF is placed between transparent antennas and rectifying circuit or antenna with the property of harmonic

rejection is designed. Among various types of transparent antenna used in rectennas, meshing microstrip patch antennas are gaining popularity for use in wireless applications owing to their low profile, lightweight, low production cost, and being conformable to planar, simple, and inexpensive to manufacture using modern printed circuit technology [58].

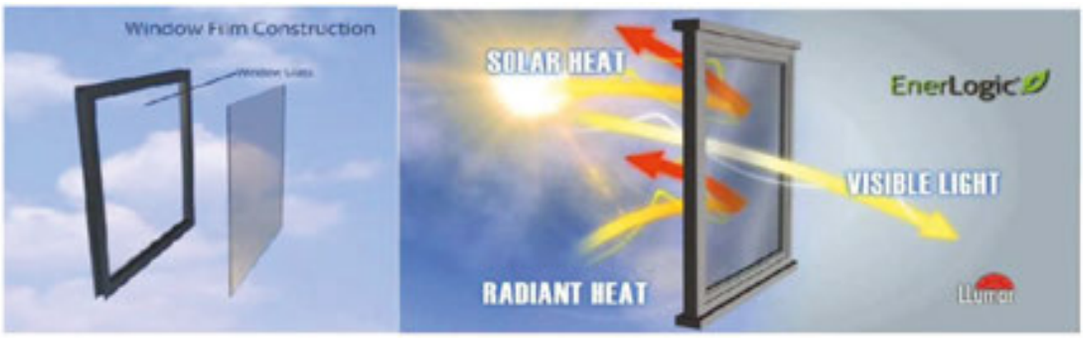

Figure 10. Transparent conductive oxide films used for sun shielding from harmful UV rays.

Figure 10 shows a typical structure of energy harvesting-enabled wireless sensor platform. A converter/a transducer convert the ambient energy forms to DC power and store the converted energy in energy storage devices as a battery or a super capacitor. A power management unit (PMU) maximizes the collected power level through matching and duty-cycle optimization in a power-efficient way. The lifetime of the power sources, such as a battery, can be increased by introducing energy harvesting systems that effectively recharge periodically the main power source or function as an additional source itself. Batteryless or battery-free autonomous operation when the main PMU can be also removed when there is a sufficient energy to drive the whole system for a truly standalone [58]. While for transparent antenna, the radiating element and ground plane are both designed using transparent conductive oxide polymer AgHT-4 while the substrate is made of glass. Recently, there has been increasing interests on the investigations of the new types of antenna designs using transparent materials. Other types also could be integrated with solar cells to reduce the surface area of small satellites [59].

6.4. Different antenna configurations in academia

Different published papers are presented in this section to describe different configuration of antenna used in RFEH. By using two orthogonal coupling slots, both as shown in **Figure 11**, linear polarizations are addressed [60]. This increased the applicability of the antenna to different incoming polarizations. The antenna was designed for an energy harvesting application at 2.45 GHz. Another more complex example of this approach is presented in [61], where a multilayer rectenna is designed using concentric annular rings (and a central circular patch), a slotted ground plane, and an integrated phase shifter/rectifier, all shown in **Figure 12**. Each of the resonator targets a separate frequency band, with the 900, 1760, and 2450 MHz bands being covered by the final design. The orthogonal slots in the ground plane, as in the last discussed design, ensure acceptance of additional signal polarizations. The phase shifter permits coherent signal combination for increased charge collection as shown in **Figure 12**.

Controlled metal spacing is also used in another fashion: parasitic gap-coupled antenna elements [62]. In this scenario, a center patch is the only radiating element fed, and two parasitic patches of differing dimensions are positioned near the main element in the same plane (see **Figure 13**). **Figure 14** shows the 3D radiation pattern for center-fed circular patch.

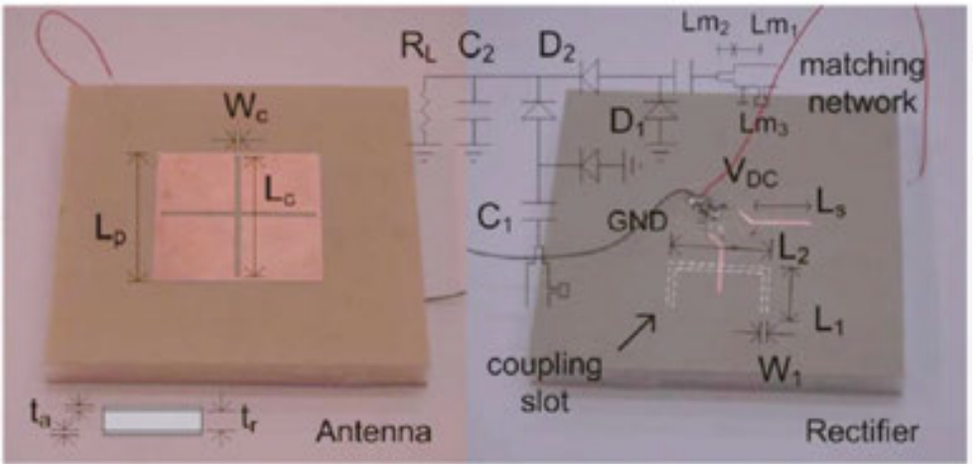

Figure 11. Cross-shaped slot-coupled rectenna.

Figure 12. Slot-coupled multiresonator (tri-band).

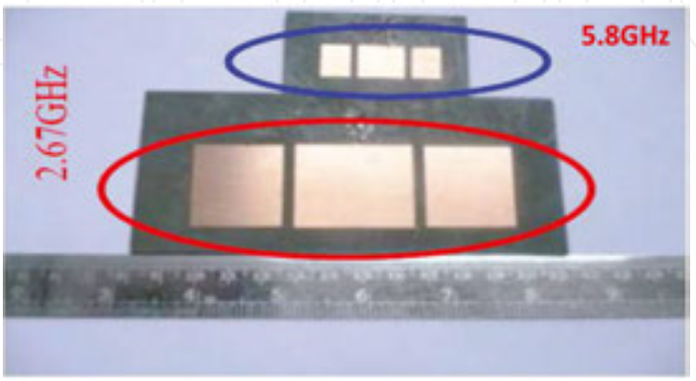

Figure 13. Two gap-coupled microstrip antennas.

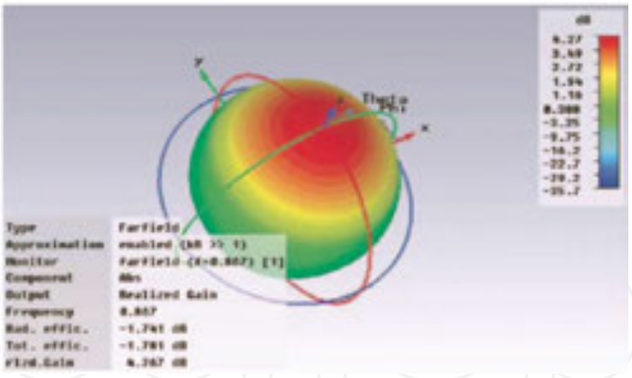

Figure 14. Radiation for center-fed circular patch.

The major advantage in this case is an increase in gain and thus an increase in harvested power level, if the orientation of the receiving antenna with respect to the energy can be maintained. Analogous to rectangular patch antennas, circular patch antennas cover a surface area dictated by the guide wavelength(s) of interest. The resonant frequency of a circular patch antenna is given in [63] as

$$f_{r,nm} = \frac{\alpha_{nm} C}{2\pi a_{eff} \sqrt{\varepsilon_{r,eff}}} \tag{2}$$

where αnm is the attenuation, aeff is the circular patch antenna radius, and εreff is the effective relative dielectric constant. Next, we take a look at folded dipoles as shown in **Figure 15**, which have been implemented in both free space [64] and printed forms. In the free space (nonprinted) version, the author of [64] fabricated a soldered folded dipole. This implementation showed a roughly 4% increase in rectification efficiency (to 15.43%) over an equivalent loop antenna. Another type of printed antenna that has seen increasing study in recent years is the spiral antenna (see **Figure 16**) [65]. In this implementation, a 64-element array of printed spiral antennas (shown in **Figure 17**) was constructed using series and parallel connections of array elements to achieve acceptance of both left-hand circularly polarized (LHCP) and right-hand circularly polarized (RHCP) signals.

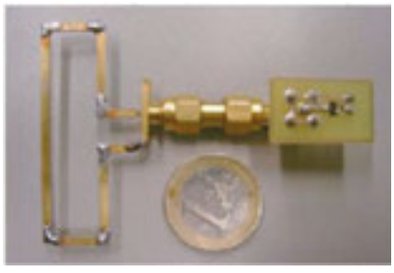

Figure 15. Folded dipole implementation at 300MHz [64].

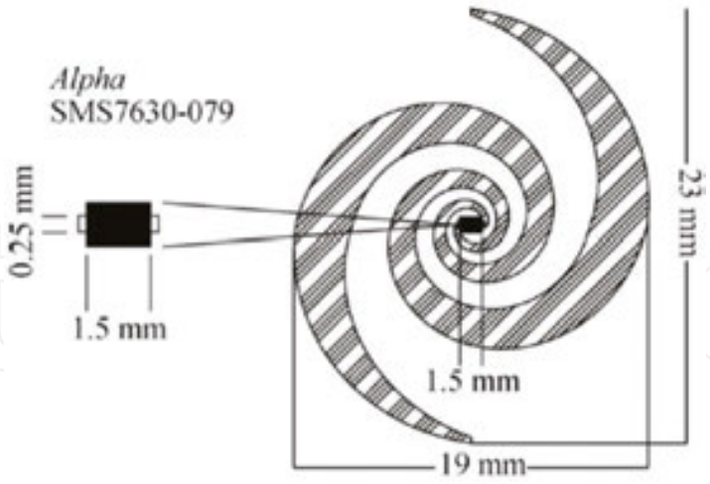

Figure 16. Single spiral antenna element.

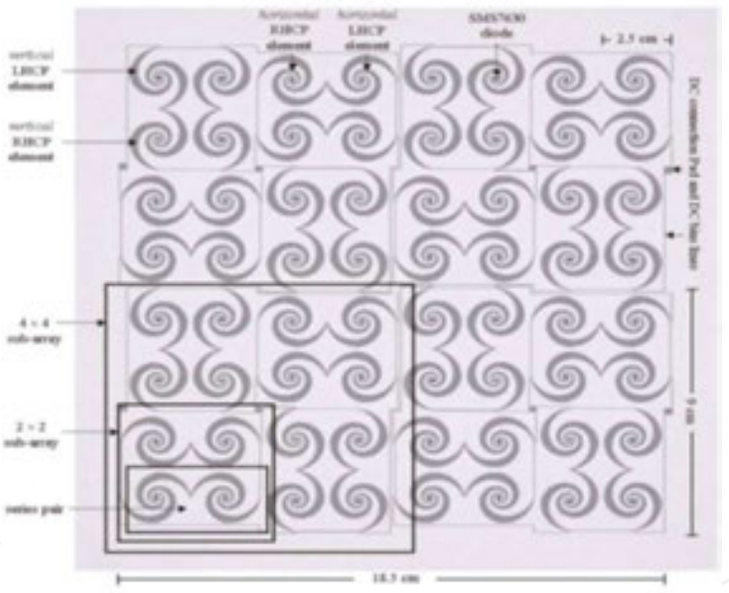

Figure 17. Array of 64 spiral antenna elements.

The authors also experimented with different DC combinations of the different rectifier outputs. The best rectification efficiency (20%) was achieved when all 4-element subarrays were connected in parallel. The total implementation was contained within a frame of 18.5 cm × 18.5 cm (34,225 mm^2). Relatively stable performance across 2–8 GHz was obtained, with test input power levels of -15.5dBm, −7.5,and 17.3 dBm. In this implementation, wideband frequency response was also shown (with minimum -10 dB return loss simulated from 1.6 to 4.0 GHz). Radiation patterns for the single element were also provided and varied with frequency but did not produce sharp gain peaks that would be nonideal for our implementation [66] as shown in **Figure 18**.

http://dx.doi.org/10.5772/64918

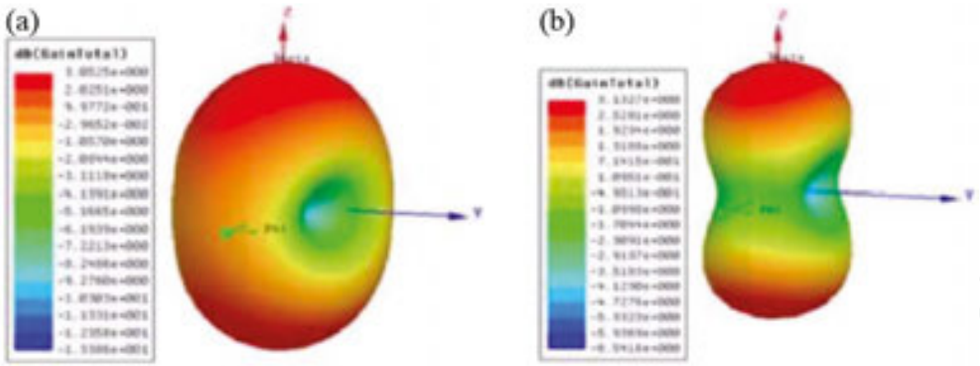

Figure 18. Spiral antenna radiation patterns at (a) 1.85 GHz and (b) 2.45 GHz.

Planar inverted-F antennas are also seeing widespread use on cellular handsets and other cellular and ISM band applications. A PIFA is in essence a raised patch antenna, shorted to the ground plane at one end (either by a pin or any width of perpendicular conductor) and fed through another pin or via at a predetermined location in the patch, based on target frequency. An example of one such antenna in an energy harvesting application can be found in [67], which targets the 2.45 GHz band. This example, illustrated in **Figure 19**, uses a full-width grounding wall (Wa = 12 mm) and contactless feeding mechanism via a feed line on the underside of the board and an aperture in the ground plane. This particular implementation was relatively narrowband, with 10 dB return loss being obtained across approximately 25 MHz, centered at 2.45 GHz. Sizing of the design was not optimized, with total dimensions of (90 cm × 40 cm × 2 cm). Evidently, construction of PIFA is more complex than a printed antenna and is susceptible to both physical variations in assembly and physical damage due to the potential fragility of both the grounding and feed point connections. Particular attention has been drawn to fractal antennas in recent years, as they see increasing use in modern designs [68]. **Figure 20** show an example of iteration common planar patch antennas based on fractal geometries. **Figure 21** shows the practical rectangular fractal patch antenna with matching network and its reflection coefficient [69].

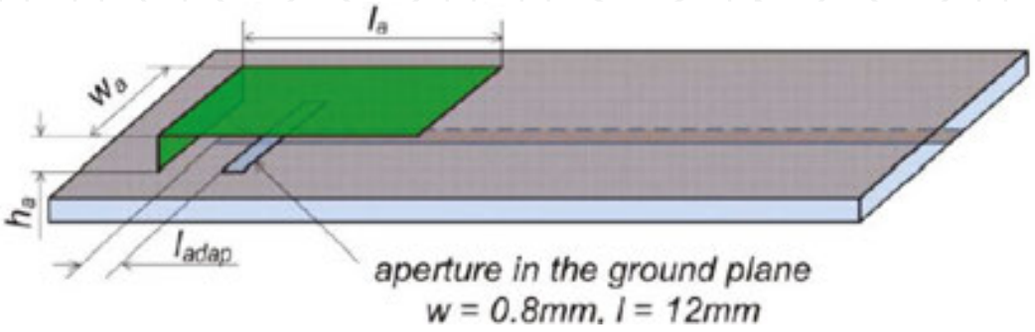

Figure 19. 2.45 GHz PIFA antenna [67].

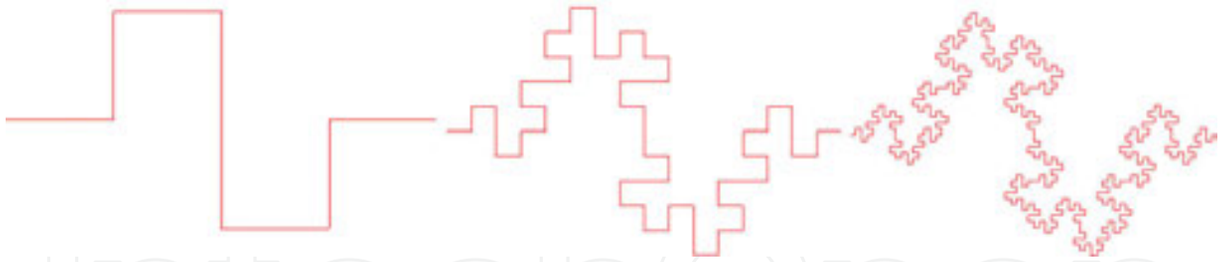

Figure 20. Minkowski sausage iterations.

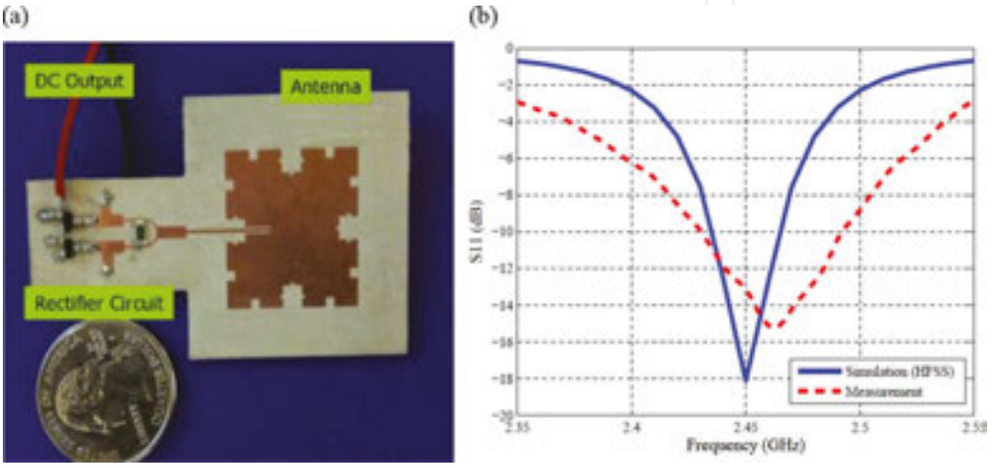

Figure 21. (a) Fabricated version of the proposed rectenna and (b) the reflection coefficient response [69].

6.5. Antenna miniaturization

Reduction of the size of the rectennas is essential these days with the rapid growth of wireless applications. Several methods have been suggested to reduce the microstrip antenna size. They include the use of thick or high dielectric constant of the substrates, modification of the basic patch shapes, short circuiting the patch to the ground plane, and other techniques that combine these three methods. The guided wavelength underneath the patch is reduced when high dielectric constant substrates are used; hence, the resonating patch size is also reduced. The reduction ratio is approximately related to $\sqrt{\varepsilon r}$. Employing high dielectric constant substrates is the simplest method of reducing antenna size but the resulting antenna exhibits narrow bandwidth, high loss, and poor efficiency due to surface wave excitation. Shorting posts have been used in different arrangements to reduce the overall dimensions of the MPA. These shorting posts were modeled and analyzed as short pieces of transmission line with a series inductance and shunt capacitance [70].

The techniques adopted to reduce the size of the antenna through geometry optimization is discussed in this section, slots with different shapes, or both of these techniques. Five miniaturized designs are shown in **Figure 22**. **Figure 22(a)** introduces a circular patch antenna with unbalance slots placed on the diameter line with 45° counter clockwise rotation of the vertical

http://dx.doi.org/10.5772/64918

diameter with different size and position relative to the center of the circular disk. The circular microstrip disk with introducing slots in antenna is resonate at 2.45 GHz, the antenna radius is reduced from the calculated result of 16.5–15.5 mm of the proposed one, yielding size reduction by 12% from original size [71]. **Figure 22(b)** shows a square-aperture-coupled patch antenna with a cross-shaped slot etched on its surface that achieved a patch size reduction of 32.5 %. The cross-shaped slot at the patch surface is etched to reduce the rectenna size due to the use of a [72]. A two-port, meandered, square patch antenna with 40 slits on the perimeter, 10 on each side, is investigated at **Figure 22(c)** to achieve 48% reduction in size. Each pair of slit is symmetrically placed with respect to the center of the side where it belongs. The current is disturbed due to the slits flowing on the surface, forcing them to meander, and thus increasing the electrical length of the patch antenna in both dimensions. So, the operating frequency decreases, whereas the physical size of the patch is unaffected. As well as, operation at a fixed frequency with reduced size is possible by increasing the slit length [73].

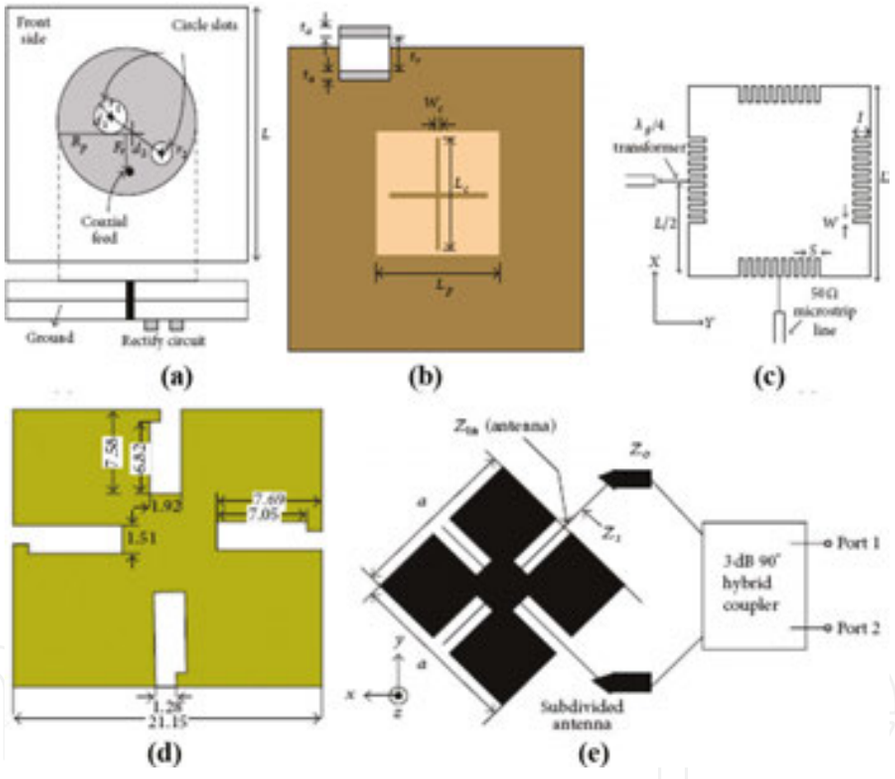

Figure 22. Various miniaturized antenna designs.

Two orthogonal pairs of irregular and unsymmetrical slits are etched on the square patch, shown in **Figure 22(d)**. The presence of slits in this antenna is a way to increase the surface current path length compared with that of the original square MPA and to reduce the size to 40% [74]. The antenna shown in **Figure 22(e)** consists of the interconnection of four corner patches sequential with four strips, and a fifth central patch representing a surface reduction of 60% [75]. The aforementioned designs were reduced by modifying the basic patch shapes and embedding suitable slots in the radiating patch. **Table 6** briefly does the comparison of

Figure 22 on the basis of changes done on their basic shape and their corresponding percentage of size reduction, whose detailed description is present in [76], respectively.

Figure 22	Shape	Frequency	Substrate	Conversion efficiency
(a)	Circular patch with slots placed on the diameter	2.45 GHz	FR-4 substrate (εr = 4.4)	12
(b)	Square patch with cross-shaped slot etched on its surface	2.45 GHz	Two Arlon A25N substrates separated by foam layer	32.5
(c)	Forty slits on the perimeter of a square patch	2.36 GHz	Taconic, TLY-5 laminate (εr = 2.21)	48
(d)	Square patch with two orthogonal pairs of irregular, unsymmetrical slits	GPS	RT/duroid 6010 LM substrate (εr = 10.2)	40
(e)	Patches alternating with four strips and a fifth central patch	5.85 GHz	RT/duroid 5870 substrate (εr = 2.33)	60

Table 6. Various antennas shapes and size reduction.

6.6. Harmonic rejections

The electronic circuits that used rectifier are used in rectennas to convert the AC current induced in the antenna by microwaves to DC current. The nonlinear components of rectifying circuits, such as diodes, generate harmonics of the fundamental frequency. These unwanted harmonics cause reradiation of the harmonic signal and electromagnetic interference with nearby circuits and antennas and reduce efficiency.

Therefore, to suppress these harmonics of microwave components, such an LPF must be added between the antenna and the diode so that the system performance is improved and prevented harmonic interference. For harmonic-rejecting antennas, different shapes of rectenna designs have been designed to reduce the MPA size and cost by removing the prerectification filter. In addition, the insertion loss at the fundamental frequency associated with it can be eliminated and increase the circuit efficiency. While the harmonic rejection antenna have also many advantages of low cost, simpler design, and conversion efficiency enhancement. Some of the designs having the behavior of harmonic rejection are shown in **Figure 23**. **Figure 23(a)** is similar to **Figure 22(a)**, where the unbalanced slot can achieve more harmonic rejection too by omitting the requirement of LPF. The diode of rectenna with square MP antenna operating at 2.4 GHz creates harmonics such as 4.8 and 7.2 GHz but a microstrip circular sector antenna with a circular sector angle of 240° and a feeding angle of 30° from the edge of the circular sector as shown in **Figure 23(b)** blocks these harmonics from reradiation [29].

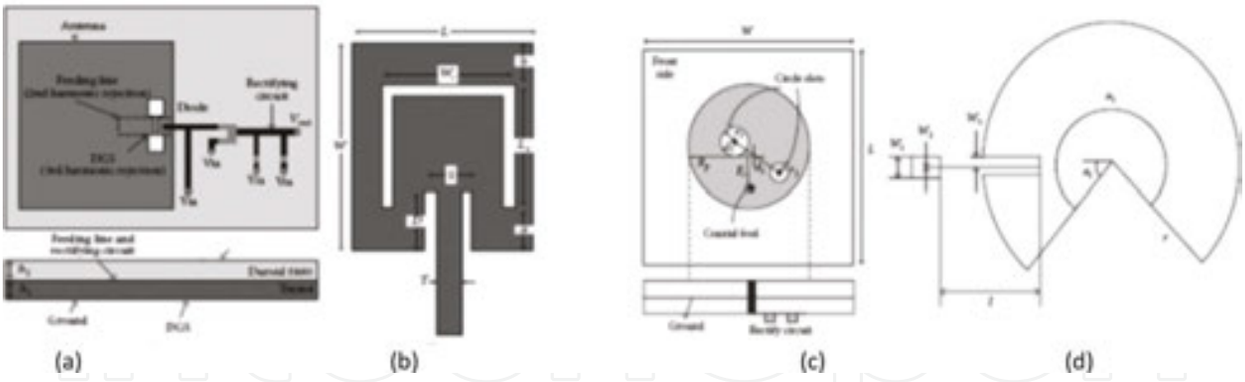

Figure 23. Various antenna designs for harmonic rejection.

Rectangular patch antenna with dumbbell-shaped slot as defected ground structure (DGS) on the ground plane resonating at 2.45 GHz as depicted in **Figure 23(c)** with reflection coefficient |S11| of −1.95 and −1.75 dB at the harmonic frequencies 4.9 and 7.35 GHz, respectively. **Figure 23(d)** is an inset-fed U-slot that resonates at 2.4 GHz, which exhibits high reflection coefficient at the second and third harmonics. The inset length not only causes deep resonance of the antenna in the desired frequency but also suppresses harmonics increasing the efficiency of the system [77]. It is also seen that along with rejecting harmonics, the antennas have higher gain than the conventional antennas in **Figure 23**. **Table 7** shows the comparison made between **Figure 23(a)–(d)** on the basis of the harmonic rejection, their corresponding gain, and conversion efficiency.

Figure 23	Shape	Frequency	Harmonic/rejection	Gain	Conversion efficiency
(a)	Circular patch with slots on the diameter	2.45 GHz	Unbalanced slots achieve second harmonic rejection	3.36 dBi CP gain	Efficiency would reach 53 and 75% with 1 K resistor load under ANSI/IEEE uncontrolled and controlled RF human exposure limit, respectively.
(b)	Microstrip circular sector antenna	2.4 GHz	Circular sector antenna with sector angle of 240° and inset feeding point at 30° from the edge avoids harmonic radiation	4.677 dBi	Maximum efficiency of 77.8% is achieved with a load resistor of 150 Ω and input power of 10 dBm
(c)	Rectangular patch antenna (RPA) with DGS	2.45 GHz	An optimized length of the feeding line and DGS are used to reject the second and third harmonics	6.4 dB	Conversion efficiency is 74% using a 1300 Ω load resistor at a power density of 0.3 mW/cm^2
(d)	U-shaped slot in middle surface of inset-fed RPA	2.4 GHz	U-slot antenna with inset feeding suppresses the harmonics	6.96 dBi	Not specified

Table 7. Various antenna shapes and the associated harmonic rejection [78].

6.7. Reconfigurable antennas

Design reconfigurable antennas have received much attention in RF energy harvesting models owing to their selectivity for operating frequency, tuning, and polarization. RF reconfigurability is basically achieved by dynamically switching the physical structure of the antenna by connecting and/or disconnecting different parts of the antenna structure, which interact with its radiation properties and thereby alter its RF response. The frequency diversity is the characteristic of having frequency selectivity and polarization selectivity can be termed as polarization diversity. Frequency diversity accommodates multiband or wideband frequency ranges and automatic frequency tuning. A reconfigurable MPA can achieve CP polarization among linear polarization (LP), right-hand circular polarization, and left-hand circular polarization. A multiband antenna is needed in order to avoid using two antennas and to allow transmission of video, voice, and data information. It can be realized by frequency diversity and simplifies installation.

Two different techniques are typically used to obtain wideband frequency ranges: using of stacked substrate patches and the activation of different staggered modes of the patch. The first approach incorporates a multilayered patch substrate that resonated at different frequencies. However, this approach has disadvantage as the height of the antenna increases. The second approach is achieved by using dual frequency operation by creating two modes under the patch, such as the TM10 and TM30 modes or the TM10 and TM01 modes. The MPA elements are primarily radiate LP waves; however, by using various arrangements of the feed with slight reshaped of the elements, circular and elliptical polarization can be obtained. CP can be achieved if two orthogonal modes are excited with a 90° time-phase difference between them. CP rectennas help in achieving DC voltage irrespective of rectenna rotation, thus avoiding polarization mismatch and loss. The diversity of the polarization reception is used for overcome of the effects of detrimental fading loss caused by multipath effects and for achieving a making polarization control in order to optimize the system performance.

The reconfigurable antenna is required for the inclusion of certain switching elements. These switches perform the job of connecting and disconnected different parts of the antenna. The switching job can be performed by passive and active elements as lumped elements (capacitors or inductors), RF microelectromechanical systems (MEMS), PIN diodes, or photoconductive switches. Several approaches have been explored, and various methods have been proposed for the methods of obtaining reconfigurable antennas. This section described various methods for the diversity in terms of frequency and polarization, MPA that have been used as reconfigurable rectennas. Seven different designs are introduced for either frequency or polarization diversity or both are shown in **Figure 24**. For polarization diversity, first three designs exhibit are introduced, for frequency diversity fourth and fifth designs demonstrate frequency diversity, and for both frequency and polarization diversities, the last two designs are introduced.

http://dx.doi.org/10.5772/64918

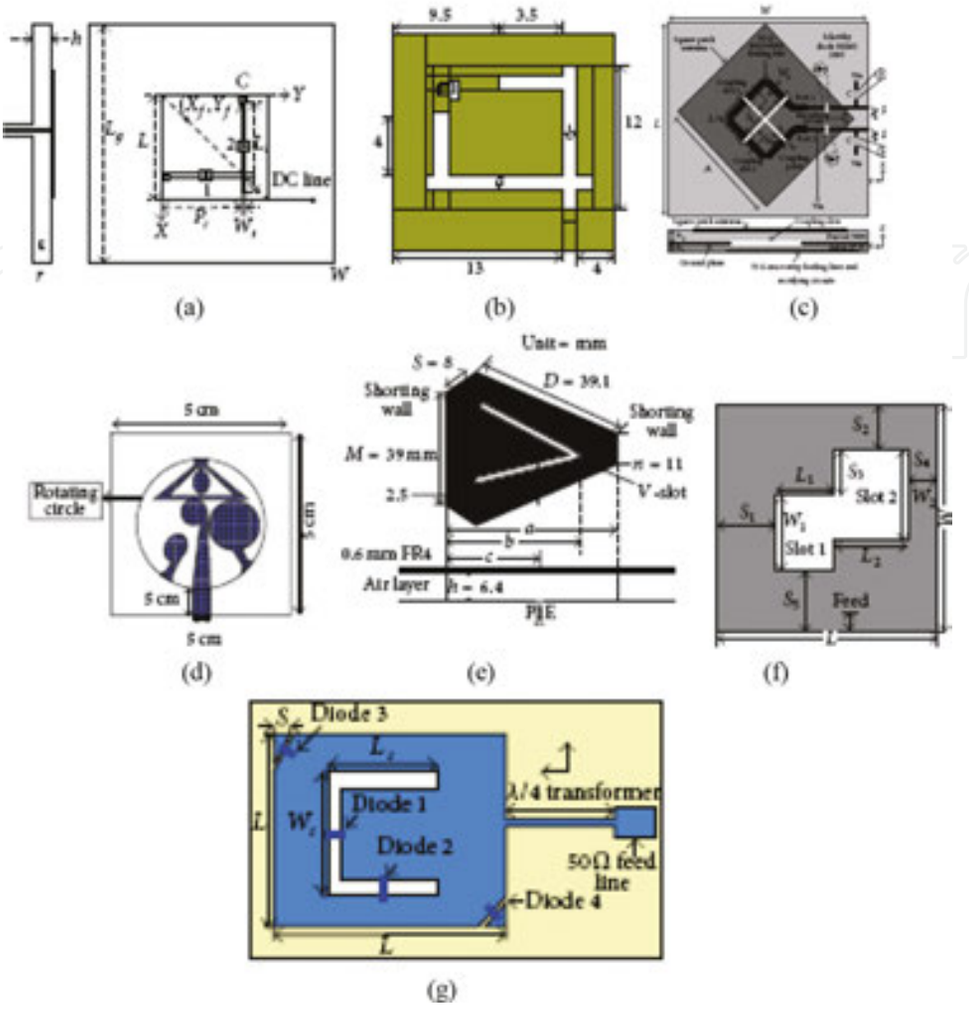

Figure 24. Various antennas design for reconfigurablility [78].

Two orthogonal slots and two PIN diodes at the center of the slot of the square MPA as shown in **Figure 24(a)** are created. The radiation fields of the TM10 and TM01 modes have the same magnitude and 90° out of phase at a midpoint frequency, generating RHCP pattern. When diode on the horizontal slot is ON and diode on vertical slot is OFF, **Figure 24(b)** shows two L-shaped slots having PIN diodes inserted in these slots of the square MPA. This design also adopts the similar way of obtaining polarization diversity, by making diodes "a" and "b" ON and OFF, respectively, for LHCP and vice versa for RHCP. The third design evaluated for polarization diversity is shown in **Figure 24(c)**. The microstrip feeding line is coupled to the square patch antenna through a cross-slot etched on the ground plane. When the excitation point is placed on port 2, the opposed coupling points on slot 2 have a peak of excitation current in phase while the opposed coupling points on slot 1 have a null of magnetic current. After a one-fourth period, the current excited is totally inverted and opposed coupling points have a null of magnetic current on slot 2 and maximum on slot 1. LHCP is then emitted, and RHCP is emitted when excitation is placed on port 1.

In **Figure 24(d)**, the diversity of resonant frequency is achieved through rotational motion of the circular patch that contains four different shapes corresponding to a different set of resonant frequencies. The different shapes are three circular patches and one slotted triangle. By the four different shapes, the four sets of frequencies are covered. For creating dual band operation (2.5–2.55 GHz), a triangular-shaped corner truncated short-circuited antenna with V-shaped slot and 3.4–3.7 GHz WiMAX bands as shown in **Figure 24(e)**. The two resonant modes are excited together by placing two shorting wall switch and a V-shaped slot in the MPA surface.

The patch antenna with both the feature of polarization and frequency diversity is introduced in the following designs. **Figure 24(f)** displays a CP MPA that can function as wireless battery charging at 5.5 GHz and data telemetry in the 5.15–5.35 GHz of wireless LAN (WLAN) band. This dual band and dual-polarized antenna is a square MPA containing two rectangular slots along its diagonal. The MPA generate RHCP by using two slots positioned along the left diagonal of and along the right diagonal to generate LHCP. The design of **Figure 24(g)** is also a MPA with frequency and polarization diversities. It consists of a corner truncated square patch incorporating U-slot and PIN diodes. Diversity of the frequency is achieved by controlling the electrical length through the PIN diode switching on the U-slot. When all diodes are OFF, it operates at resonant frequency of 2.41 GHz. It operates at 2.65 GHz in three cases: when all diodes are ON, when diodes 1, 3, and 4 are ON and diode 2 is OFF, and when diode 1 is ON and other diodes 2, 3, and 4 are OFF. Polarization diversity is achieved by switching PIN diodes ON the slot with truncated corners. If diode 2 is turned OFF and other diodes are ON, it exhibits LP characteristic. RHCP characteristic is exhibited when diode 1 is turned ON and other diodes 2–4 are turned OFF. If all diodes are ON, then LHCP is emitted [78].

6.8. Recent development (our proposed antennas)

The Electronics Research Institute has published many papers in International Periodical Journals regarding transparent or oblique antennas in RF harvesting energy. Following section describes different configurations of antennas. Multiband operations with reducing size are essential in cellular communication systems and other wireless communication applications such as WLANs, Bluetooth, and WiMAX. Among various possible antennas, planar inverted-F antennas (PIFAs) have the advantages of low profile, compact size, and very suitable for wireless communication applications in this day. The broadband characteristic of PIFA is achieved by using CPW feed, around 10% impedance bandwidth improvements over any other antenna feeding mechanism. The CPW offers several advantages over traditional microstrip line: it simplifies fabrication, it facilitates easy shunt as well as series surface mounting of active and passive devices, it reduces radiation loss, and a ground plane exists between any two adjacent lines, hence crosstalk effects between adjacent lines are very weak. Recently, meandered PIFA is widely used for creating resonant frequencies or with size reduction in mobile handset and wireless communication applications. The coupled slot is used within CPW-fed PIFA to create a new independent resonant frequency as shown in **Figure 25**.

http://dx.doi.org/10.5772/64918

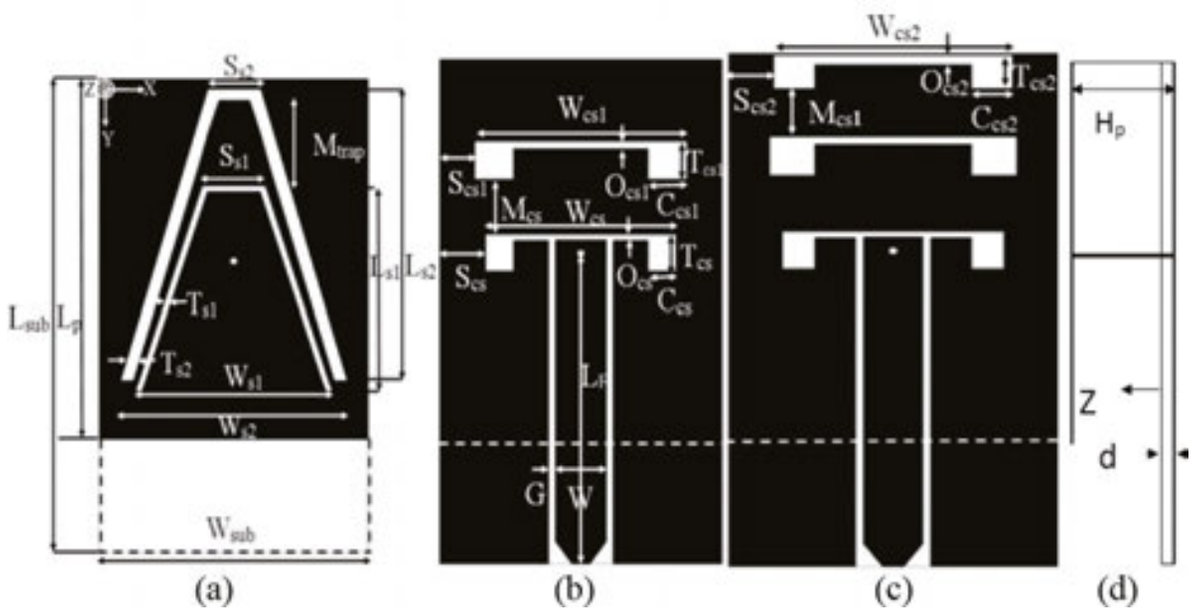

Figure 25. The geometry and configuration of (a) patch with two trapezoidal slots, (b) ground plane with dual coupled slots, (c) ground plane with three coupled slots, and (d) side view.

The functionality is not the only required demand in such antenna systems for wireless communication applications, and other characteristics should be satisfied such as small size, lightweight, omnidirectional radiation pattern, reasonable gain, acceptable impedance bandwidth, and frequency-independent operation. Usually when some parameters are adjusted to set a band to a particular frequency, the other resonances frequencies are affected, and so, the antenna has to be redesigned. However, it independently set the individual frequency bands, one by one, without affecting other bands, by applying varactor diodes with variable capacitors to electrically and independently tune the operating resonant frequencies over a wide frequency range as shown in **Figure 25** and the fabricated proposed antenna as shown in **Figure 26**, and it response is shown in **Figure 27** [79] (**Table 8**).

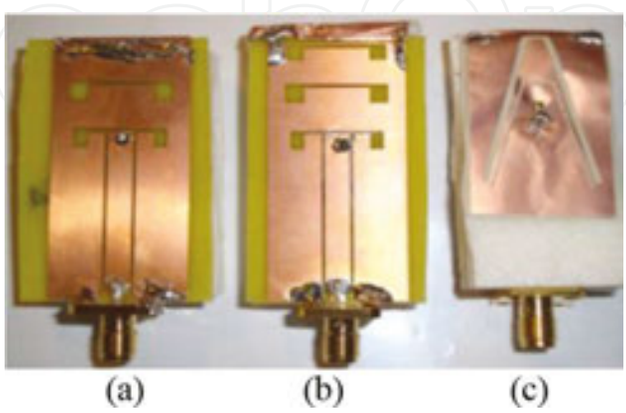

Figure 26. Photo of the fabricated antennas (a) two coupled slots, (b) three coupled slots ground plane, and (c) radiator plate.

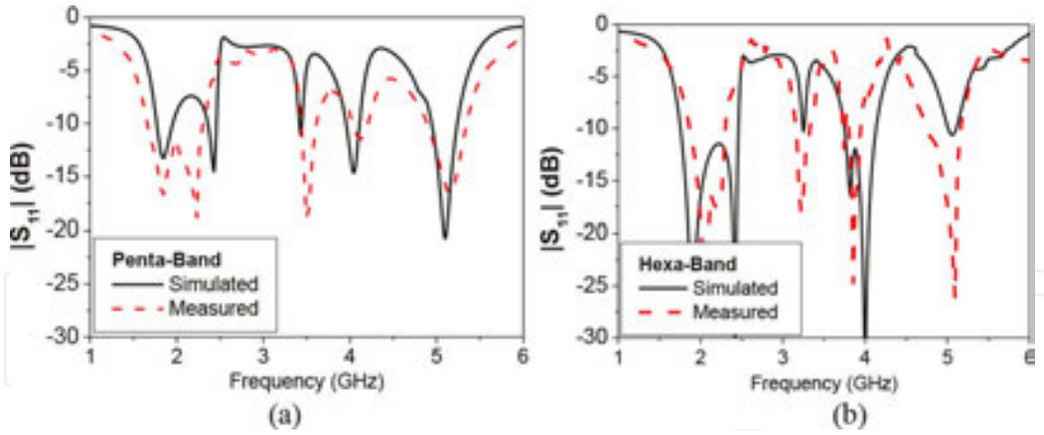

Figure 27. The simulated and measured |S11| of the proposed CPW-fed PIFA (a) pentaband and (b) hexaband.

Figure 24	Antenna shapes	Frequency GHz	Reconfigurable	Cause of reconfigurability	Application
(a)	Square patch orthogonal slots and two PIN diodes	2.64	Polarization diversity RHCP/ LHCP	By turning the diode ON/OFF. Either RHCP/LHCP can be obtained	WLANs satellite link and space robots
(b)	Square patch orthogonal L-shaped slots with two PIN diodes	4.44	Polarization diversity RHCP/ LHCP	Reconfigurability is achieved by switching two PIN diodes	Unlicensed and licensed WiMAX
(c)	Square patch coupled to microstrip line by aperture	2.45	Polarization diversity RHCP/ LHCP	Reconfigurability is obtained by selecting one of two excitation points	Not available
(d)	A circular patch to feed different shapes	Cover five 2–7	Frequency diversity	Reconfigurability is obtained by rotation motional of the part of the antenna	Cognitive radio system
(e)	Short circuited triangular patch antenna with truncated corner	2.5–2.55 and 3.4–3.7	Frequency diversity	By placing two shorting walls with a V-shaped slot patch	Covers 2.5–2.55 and 3.4–3.7 WiMAX
(f)	Two rectangular slots properly position	5.15–5.35 and 5.5	Frequency diversity and polarization	Positioning the slots along the left diagonals	Can function as a rectenna for wireless battery charging 5.5 and 5.15–5.35
(g)	Square patch with two PIN diodes on a U-shaped slot	2.415 and 2.65	Frequency diversity and polarization	The switching of the PIN diode on the U-slot realizes frequency diversity and polarization	WLAN digital multimedia broad casting

Table 8. Various antennas shapes and their reconfigurability.

http://dx.doi.org/10.5772/64918

Another sturcture is used for reconfigurable multiband PIFA as shown in **Figure 28**. The antenna is based on a combination of a CPW-fed PIFA, meander turn-shaped slot on the radiating plate [80] and coupled slot within the ground plane for multiband operation and size reduction characteristics. As the number of meander turn-shaped slots is increased, new resonant frequencies are excited. PIN diode is used to switch the fundamental resonant frequency from high to low frequency. This antenna operates over LTE band 11 (1.47–1.5 GHz), LTE band 8 (925–960 MHz), GSM1800 MHz/GSM1900 MHz/Bluetooth 2.4 GHz, WiMAX frequency range (3–4 GHz), and WLAN frequency range (5–6 GHz).

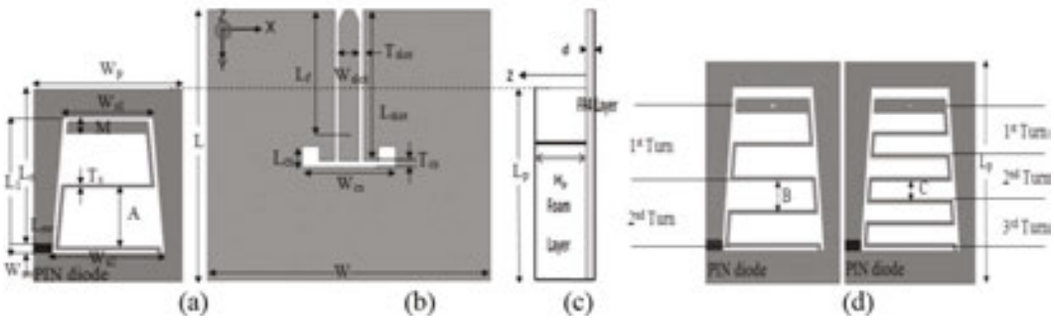

Figure 28. The geometry and configuration of CPW-fed PIFA with PIN diode switch (SW) (a) radiator with one meander turn, (b) ground plane, (c) antenna side view, (d) radiator with two meander turns, and (e) radiator with three meander turns.

The design is started by conventional CPW-fed PIFA (the meander turns shaped slot on the radiator and the coupled slot in the ground plane are removed) to operate at Bluetooth 2.4 GHz. **Figure 29** obtains the simulated |S11| of one meander turn-shaped slot with ON/OFF switch mode. First is used to show PIN diode switches with the open and close states to switch the antenna from LTE band 11 (1.47–1.5 GHz) to LTE band 8 (0.925–0.960 GHz) with total 63% size reduction as compared to the original PIFA size. The fabricated photo of the antennas are shown in **Figure 30**, the reflection coefficient for both PIN diode modes of the proposed antenna with three turns of meander slot are shown in **Figure 31(a–c)**, respectively. The concept is approved for the three designs.

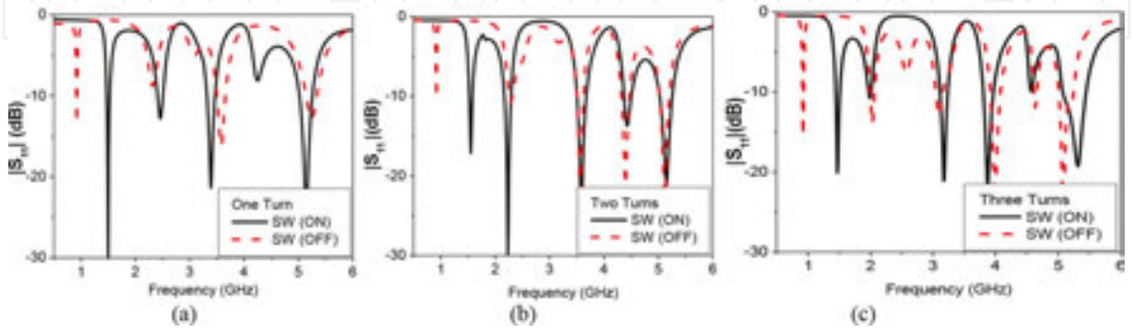

Figure 29. The simulated |S11 | of (a) one, (b) two, and (c) three meander turn-shaped slots with switch ON/OFF modes.

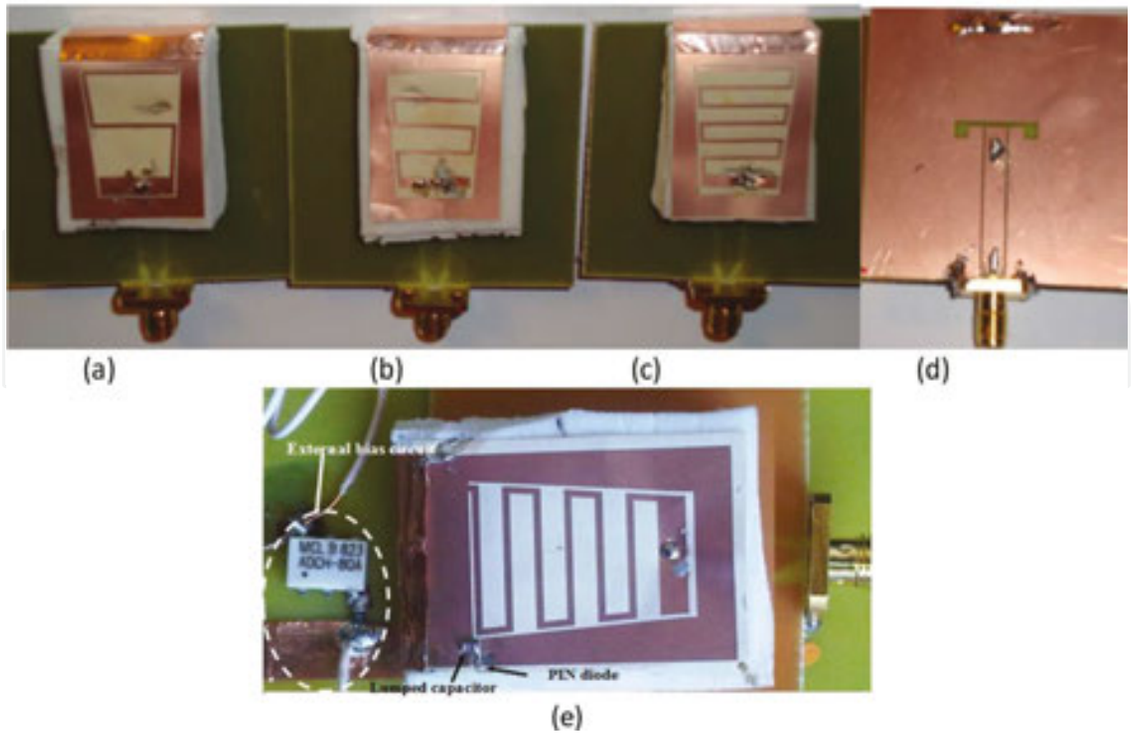

Figure 30. Photo of the fabricated proposed antennas (a) one turn, (b) two turns, (c) three turns, (d) ground plane with coupled slot, and (e) PIN diode and external biasing circuit.

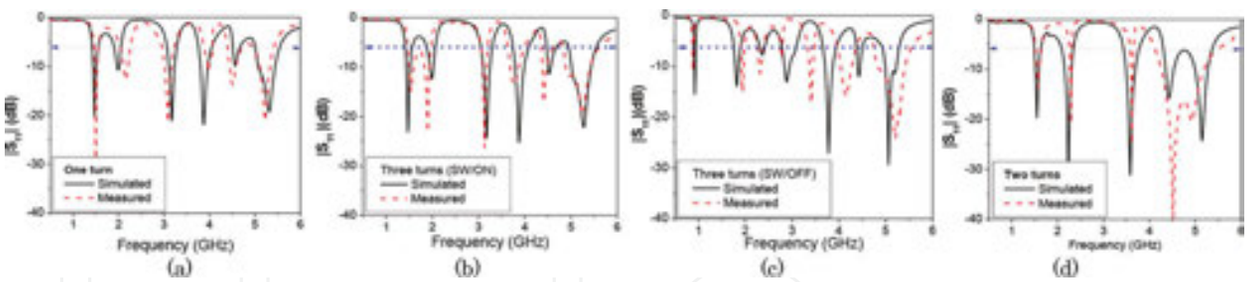

Figure 31. Comparison between simulated and measured |S11| of (a) one turn, (b) two turns, (c) three turns with SW/ON state, and (d) three turns with SW/OFF state.

The gains of antenna are in between 1.8 and 4.8 dBi at each resonant frequency with good impedance bandwidth (|S11|<-6 dB) that is suitable for standard channel bandwidth for wireless communication applications such as LTE band 8 (0.925–0.960 GHz), GSM1900, LTE band 2, LTE band 33, LTE band 11, Bluetooth, WiMAX, and WLAN. The radiation efficiency is larger than 70%, and it is decreased with switching the antenna on from high to low frequency due to ohmic losses of the PIN switches.

Another method used to achieve multiband with compact size is meta-material-inspired loading exploited to create a new resonance while maintaining the antenna's small form factor as shown in **Figure 32**.

http://dx.doi.org/10.5772/64918

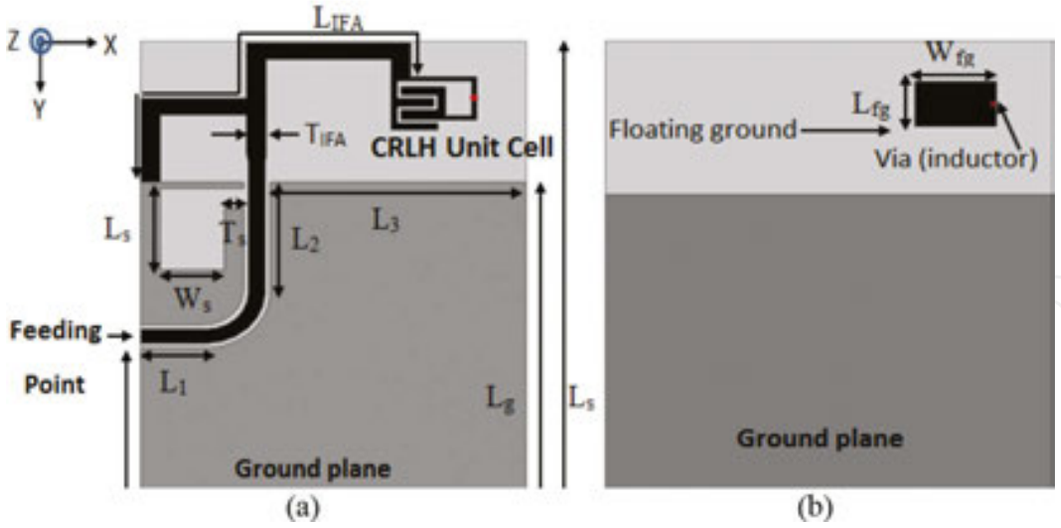

Figure 32. Geometry of triple-band MTM-inspired small USB antenna (a) top view and (b) bottom view.

This section presents two compact antenna designs using the meta-material techniques. The first design [81] consists of CPW printed IFAs loaded with CRLH unit cells to achieve new operating bands with the same antenna size beside the fundamental resonant frequencies of IFA arm itself.

A "defected" ground plane is formed by appropriately cutting a dumbbell-shaped slot out of the CPW ground plane to create extra resonant frequency. The proposed antenna design consists of two IFA arms loaded with two TL-MTM unit cells to create new two operating bands in addition to the operating frequencies of two IFA arms themselves for USB applications. The geometry with detailed design parameters of the proposed triple-band USB antenna is shown in **Figure 32**. The simulated S parameters of the design procedures are shown in **Figure 33**, starting with the single CPW-fed IFA that is designed to cover lower WLAN application and then used the CRLH meta-material-inspired cell to create the second resonant frequency to cover WI-MAX 3.5 GHz application. The antenna size reduced by around 22% from the fundamental resonant frequency of the printed F antenna. Finally, the slot is etched within the ground plane to cover the upper WLAN application (5.2–5.25 GHz).

The −10 dB antenna exhibits bandwidth of 200, 100 and 80 MHz for lower WLAN 2.4 GHz band, WiMAX 3.5GHz band, and upper WLAN 5.2 GHz band, respectively. These results agree well with simulation results as shown in **Figure 33**. The simulated gains are 2.3, 2.1, and 2 dBi at 2.4, 3.5,and 5.2 GHz, respectively with radiation efficiency more than 75%. The theory of loading two arms CPW-fed IFA with two CRLH unit cells was explained and verified using the RLC-lumped components of the simulators, advanced designing system (ADS), and high-frequency structure simulation (HFSS), and there is good agreement with the measured result, to be used for mobile and wireless data USB applications. The whole geometry with detailed design parameters of the proposed triple-band USB antenna is shown in **Figure 34** [82]. The photo of fabricated proposed antenna and measured results are shown in **Figure 35**. Measured impedance bandwidths (−6 dB) for each resonance are suitable for the channel bandwidth of

the LTE band 11 (1.42–1.47 GHz), GSM1800 (1780–1890 MHz), Bluetooth (2.4–2.45 GHz), WiMAX standards (3.4–3.5 GHz) and (3.7–4 GHz), and upper WLAN (5.2–5.25 GHz). The measured realized gains at four resonant frequencies are 2.8, 1.9, 3.1, and 2.1 dBi, respectively. The radiation efficiency was measured by using Wheeler cap method. The average radiation efficiency is more than 75% [83].

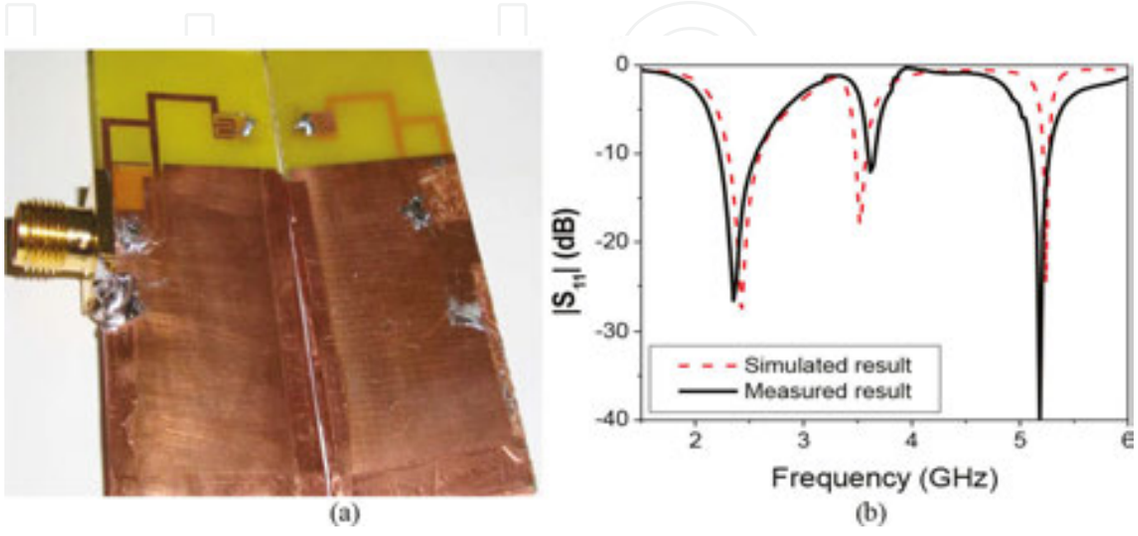

Figure 33. (a) Photo of the fabricated USB antenna and (b) the |S11 | comparison of the simulated and measured results.

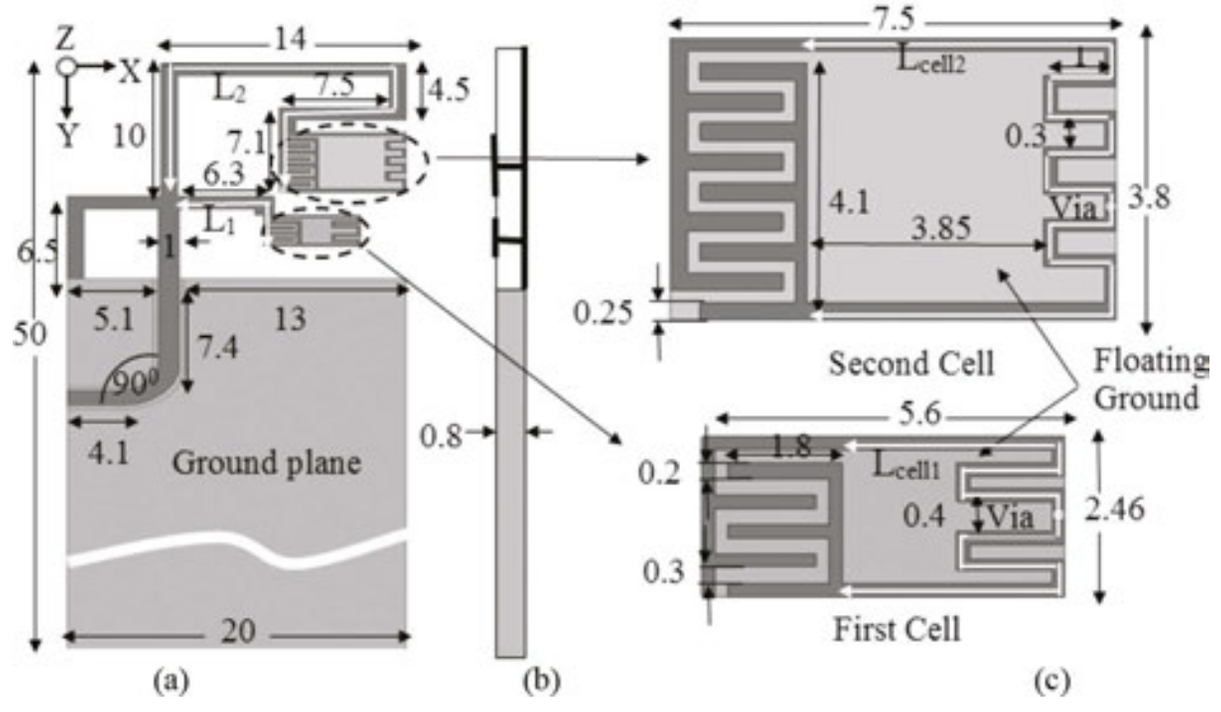

Figure 34. Quad band CPW-fed printed IFA antenna with two meta-material-inspired unit cells (all optimized dimensions are in mm) (a) top view, (b) side view and (c) two CRLH unit cells.

http://dx.doi.org/10.5772/64918

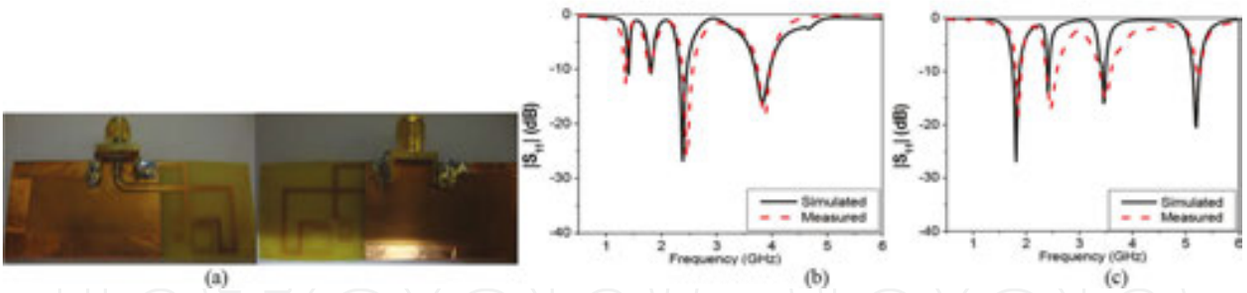

Figure 35. (a) The fabricated antenna, (b) simulated and measured |S11| of implemented antenna (1.4, 1.8, 2.4, and 3.8 GHz), and (c) optimized antenna (1.8, 2.4, 3.5, and 5.2 GHz).

6.9. Tunable design

The aim is to tune the operating frequency of the antenna and to have a single multifunctional antenna in a small terminal for many applications. Varactor diodes are the most commonly used technique to tune the operating frequencies in RF and front-end applications. A DC block capacitor, CDC = 100 nF, between the short and the ground is needed as shown in **Figure 36**. The capacitor CDC generates an open circuit for the DC voltage and a short circuit for the RF signal. An inductor of 1 μH is used to support complete path to the ground plane in the DC case [84, 85]. The comparisons between simulated and measured results are shown in **Figure 37**. The fabricated antenna with two different voltages V1 and V4 are shown in **Figure 38**.

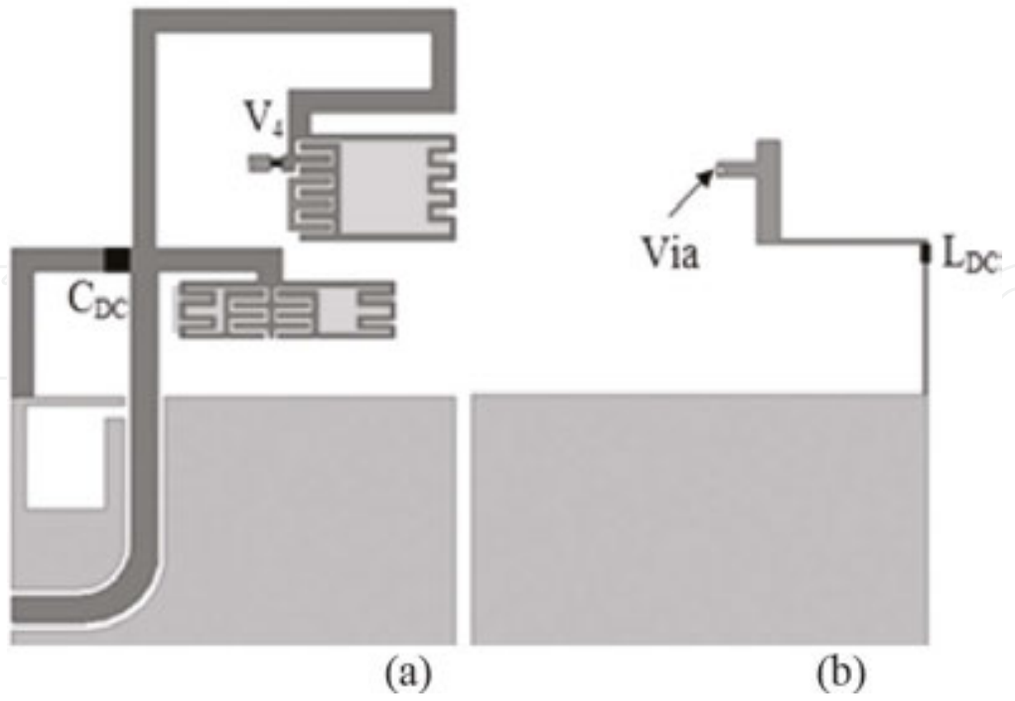

Figure 36. The proposed antenna with DC biasing network (a) top view and (b) back view.

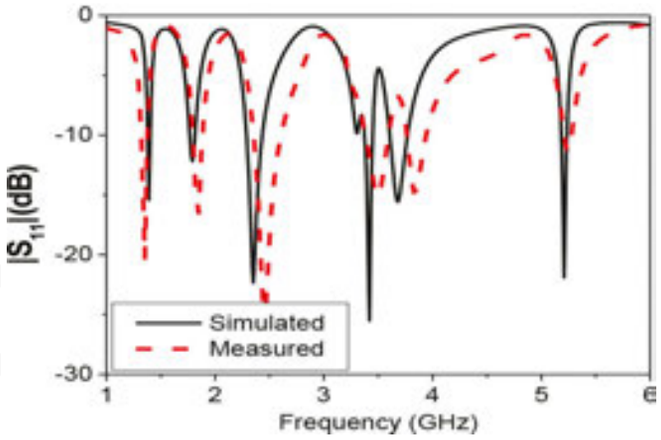

Figure 37. The simulated and measured |S11| of the proposed antenna with package of PVC casing material.

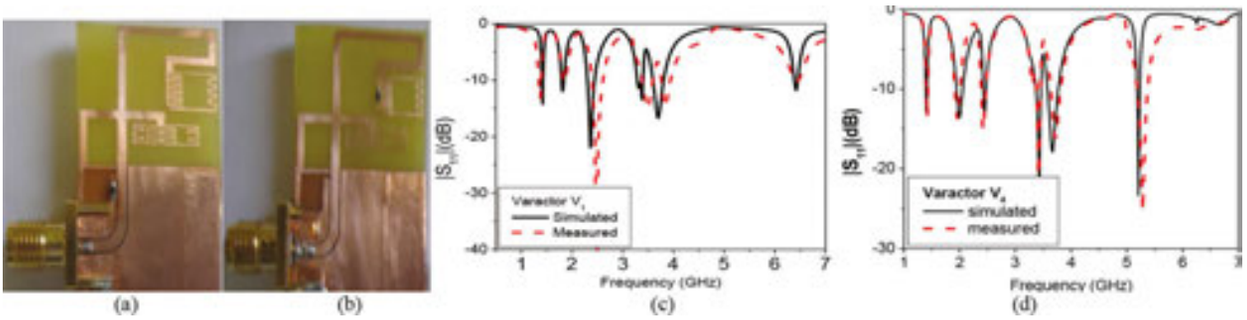

Figure 38. The photo of the fabricated USB antenna with 0.05 pF (a) varactor V1, (b) varactor V4 and the simulated and measured |S11| with varactors (c) V1 and (d) V4.

7. Nanoantennas

Approximately 30% of this incident Sun energy is reflected back to space from the atmosphere, atmospheric gases absorb 19% and reradiated to the Earth's surface in the mid-IR range from 7 to 14 μm and 51% is absorbed by the surface and reradiated at around 10 μm. The energy incident in both the visible and IR regions to the earth is reradiated IR energy underutilized by current technology.

Several approaches have been used to successfully harvest energy from the Sun and conversion of solar energy to electricity using photovoltaic cells. In addition to photovoltaics is the optical rectenna, which is a combination of a rectifier and a receiving antenna. The initial rectenna concept was demonstrated for microwave power transmission by Raytheon [86]. This illustrated the ability to capture electromagnetic energy and convert it to DC power at efficiencies approaching 84%. Most of the papers have been performed to extend the concept of rectennas to the infrared and visible regime for solar power conversion. While the progress have been made in the fabrication and characterization of metal-insulator-metal diodes for use in infrared

rectennas [87]. The optical antennas has been demonstrated, which can couple electromagnetic radiation in the visible regime in the same way as radio antennas do at their corresponding wavelengths [88]. The development of economical manufacturing methods for large-scale fabrication of nanoantenna-based solar collectors becomes the challenge. It needs to improve the efficiency of rectification of antenna-induced terahertz (THz) currents to a usable DC signal, and material properties and behavior of antennas/circuits in the THz solar regions need to be further characterized.

7.1. Photovoltaic limitations

To begin with the p-n junction solar cell is utilized for solar energy harvesting technologies. After this, the physics of energy absorption is used and carrier generation are the function of the material characteristics and corresponding electrical properties as photonic band gap. In order to excite an electron from the valence band into the conduction band, a photon needs only to have greater more than that of the band gap. However, the frequency solar spectrum approximates a black body spectrum at ~6000 K, and much of the solar radiation reaching the Earth is composed of photons with energies greater than the band gap of silicon. By the solar cell, these energy photons are absorbed but the difference in energy between these photons and the silicon band gap is converted into heat rather than into usable electrical energy. For a single-junction cell, this sets an upper efficiency of ~31% [89].

7.2. Alternative economical PV

Developing of another energy harvesting approach based on the use of nantennas to absorb incident solar radiation was founded. Moreover of PVs, which are quantum devices limited by material band gaps, antennas are resonated at natural resonance frequency and the bandwidth of operation is a function of physical antenna geometries. Nantenna electromagnetic collectors (NECs) can be formatted as frequency selective surfaces to efficiently absorb the entire solar spectrum. Contrastingly, by generating single electron-hole pairs, such as the PV case; a time-changing current in the antenna brought on by the incident of the electromagnetic field from the sun. Collection efficiency of the incident radiation is dependent upon proper design of resonance and impedance matching of the antenna [90].

7.3. Nanoantennas theory

The antennas theory is that the incident light on the antenna causes electrons in the antenna to move back and forth at the same frequency as the incident light. This is done by the electric field oscillating of the incoming electromagnetic wave. The movement of current electrons alternates in the antenna circuit and then converts itself into a direct current. The AC must be rectified, which is typically done with some kind of diode [91–96]. As shown in **Figure 39**, the obtained DC can then be used to power an external load. According to simple microwave antenna theory, the antenna resonant frequency (which results in lowest impedance and thus highest efficiency) scales linearly with the dimensions of the antenna. The solar spectrum wavelengths lie between approximately 0.3 to 2.0 μm. However, in order for a rectifying antenna to be an efficient electromagnetic collector in the solar spectrum, it needs to be on the

order of hundreds of nanometer in size. This can be achieved by shrinking the dimensions of the antenna to the scale of the wavelength. For this reason, nantennas are used as an alternative to scale the microwave theory down to the IR regions of the electromagnetic spectrum in **Figure 39** [97].

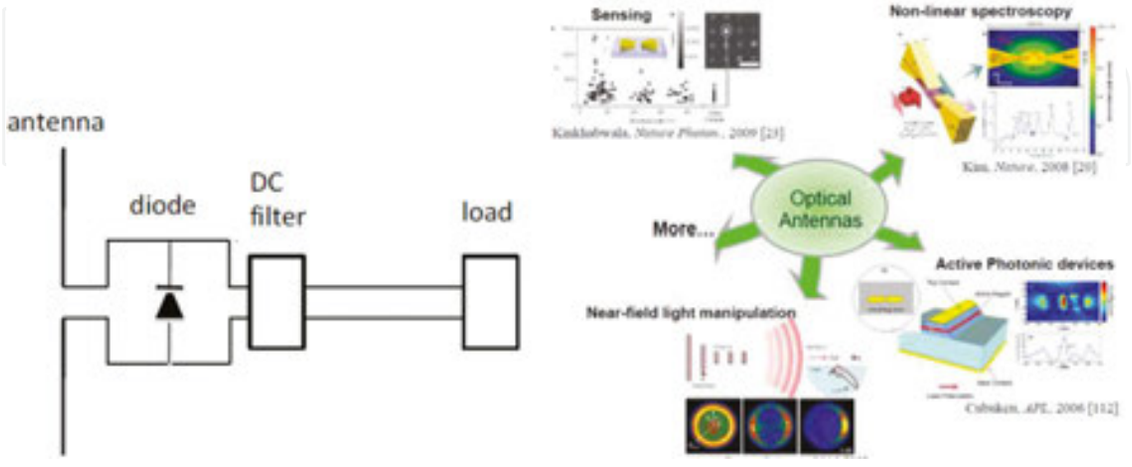

Figure 39. A wide range of applications are driving the research in optical antennas. The applications reported in recent years include biological and chemical sensing, nonlinear spectroscopy, high-harmonic generation, and solar energy harvesting.

Cyclic plasma induces when an antenna is excited into a resonance mode of free electrons that is movement from the metal antenna. The electrons freely flowing straight in to the antenna are oscillating current at the same frequency as the resonance. The current flow crossed the antenna feed point in a balanced antenna; the feed point is located at the point of lowest impedance as in **Figure 40**. The e-field is clearly concentrated at the center feed point, this provides a convenience point to collect energy and transport it to other circuitry for conversion. Nanoantenna structure incorporates an antenna layer, a dielectric standoff layer, and a ground plane as in **Figure 41**. It is found that in right shape, materials, and size, the simulated nantennas could harvest up to 92% of energy at infrared wavelength. The operation of optical frequencies, an ultrafast diode rectifies the optical frequency signal absorbed by the antenna, producing a DC voltage. The configuration shown is a clamping circuit that theoretically provided 100% conversion efficiency as a traditional rectifier. The way to use the rectified DC energy is to connect a load with a low-pass filter directly across the diode. The performing of a classical circuit analysis is the output: DC voltage, at the load can be high with the peak input AC voltage across the antenna [86]. The total efficiency of nanorectennas consists of two parts. The first part is the efficiency by which the light is captured by the nanoantenna and brought to its terminals. The second part is the efficiency by which the captured light is transformed into low-frequency electrical power by the rectifier. The radiation efficiency of IR for five different conducting materials silver, gold, aluminum, copper, and chromium, respectively, are reported in vacuum. Copper efficiencies reach to 60–70% but the bandwidth is rather limited. This is reflected in the total efficiency that reaches a maximal value of almost about 30% for a dipole length of 300 nm [97].

http://dx.doi.org/10.5772/64918

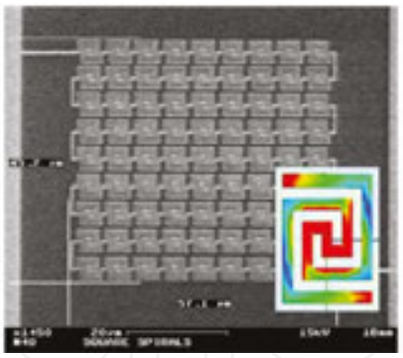

Figure 40. Array of loop nanoantennas, (inset) flow of T Hz current to feed point of antenna. Red represents highest concentrated e-field.

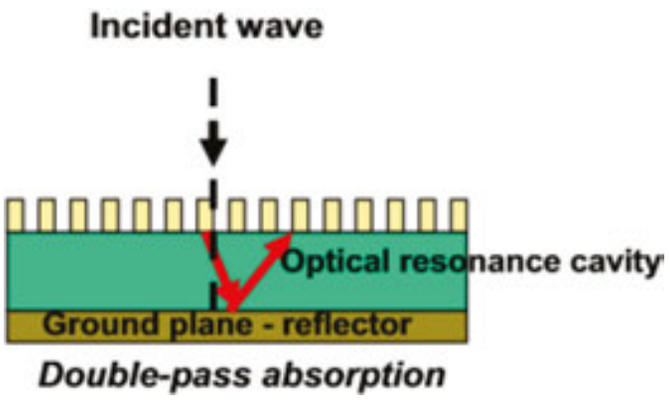

Figure 41. Side walls of nanoantenna showing path of incidence of wave.

The nantenna captured the electromagnetic energy from both solar radiation and thermal earth radiation. As shown in **Figure 42**, various self-complementary antennas used as dipoles, spirals, loops, etc. are the candidates due to their inherit wide bandwidth and feed point configurations for concentrating energy collection, and the antenna element size is related to the wavelength of light harvest.

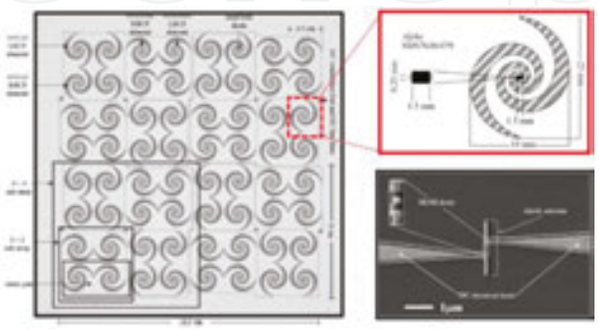

Figure 42. Array of square spiral nanoantennas.

The concept was performed using spiral antenna structures as shown in **Figure 43**. It shows that a modeled thermal energy profile indicating that the e-field is clearly concentrated at the center feed point.

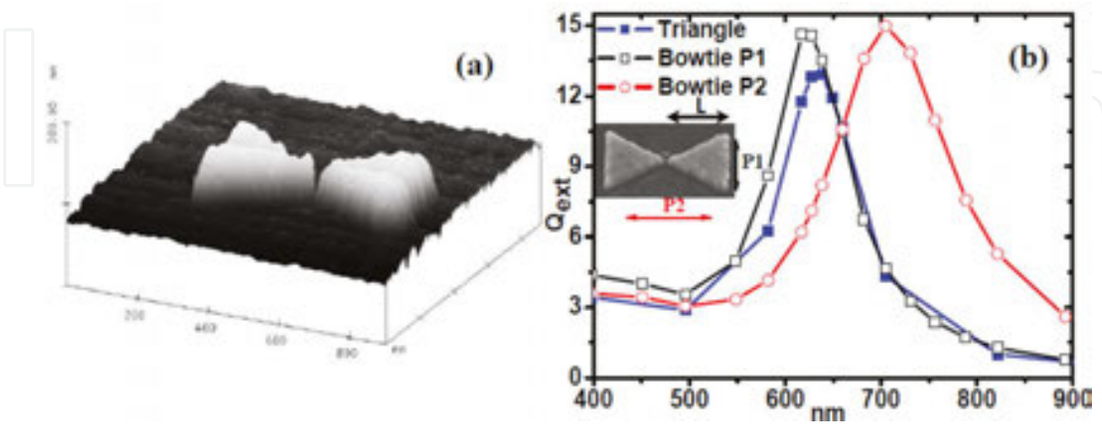

Figure 43. (a) Topographic image of a 120 nm Au bow tie antenna with 20 nm gap fabricated using electron-beam lithography and (b) DDA-simulated extinction efficiency showing polarization dependence and splitting of triangle resonance mode into two orthogonal modes for the bow tie dimer (L = 120 nm).

The nantenna radiation pattern displays the angular reception characteristics that result in a wider angle of incidence exposure to radiation than a typical PV device. The flux is collected from the Sun, which falls within the radial beam pattern of the antenna. It reduce the need of the mechanical solar tracking mechanisms that are a critical antenna characteristic that optimizes the energy collection from the Sun as it pass throughout the sky. There is another mechanism for increasing the efficiency of antenna arrays through the expansion of the radial field. Antennas do not provide a means of converting the collected energy, so this will need to be accomplished by associated circuitry, such as rectifiers. The virtual large surface area antenna focuses the electromagnetic energy onto the nano-sized energy conversion material fabricated at the antenna feed point. Theoretical efficiency is improved by the enhanced radiation capture area of the antenna. When efficiency compared to the theoretical of single junction solar cells (30%), nantennas appear to have a significant advantage. The advantage nantennas has over semiconductor photovoltaics is that nantenna arrays can be designed to absorb any frequency of light.

The nantenna resonant frequency is selected by varying its length. In order to absorb different wavelengths of light, different band gaps are needed. In order to vary the band gap, the semiconductor must be alloyed or a different semiconductor must be used altogether. Nantennas exhibit potential advantages in terms of polarization, tunability, and rapid time response. (i) they have very small area detection, (ii) their electromagnetic field allows localization beyond the diffraction limit, (iii) they very efficiently release radiation from localized sources into the far field, (iv) they make possible the tailoring of the interaction of electromagnetic field at the nanoscale, and (v) they could be tuned to a specific wavelength [89].

http://dx.doi.org/10.5772/64918

7.4. Applications

Large-scale economical fabrication is used for covering the roofs of buildings and supplementing the power grid. It collects different separate bands of electromagnetic energy. By using double-sided panels, a broad spectrum of energy from the sun during the day could absorbed while the other side might be designed to take in the narrow frequency of energy produced from the earth's radiated heat or residual heat from electronic devices as shown in **Figure 44**. This technology may also support several applications, including passive thermal management products, such as building insulation, window coatings, and heat dissipation in electronic consumer products, such as computers. These types of antennas are broadband collectors of energy with a spectral emission response. This generates a frequency-selective distribution of energy that potentially collected unwanted energy residual or incident heat and redistribute it at other innocuous wavelengths. Other applications are conceivable that nantenna collectors, combined with appropriate rectifying elements, could be integrated into the "skin" of consumer electronic devices to continuously charge their batteries.

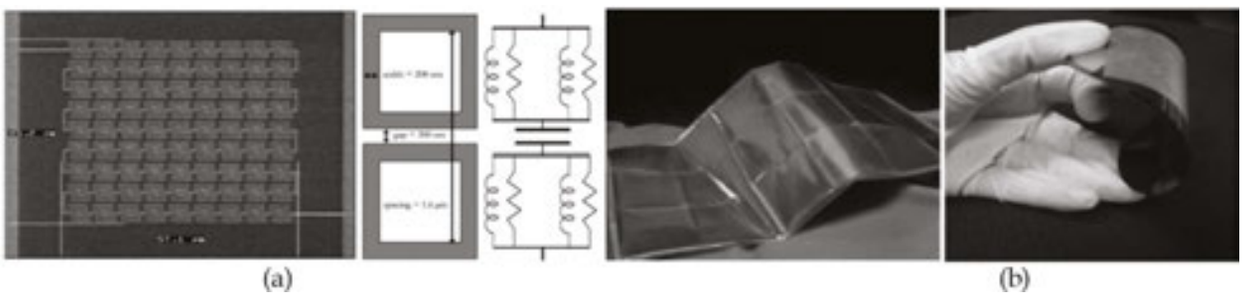

Figure 44. (a) SEM image of the square loop antenna array and (b) nanoantenna collector sheet.

Author details

Dalia M.N. Elsheakh

Address all correspondence to: daliaelsheakh@gmail.com

Electronics Research Institute, Giza, Egypt

References

[1] H.J. Visser, A.C.F. Reniers, and J.A.C. Theeuwes, "Ambient RF energy scavenging: GSM and WLAN power density measurements," IEEE 38th European Microwave Conference, Amsterdam, Netherlands. pp. 721–724, October 27–31, 2008.

[2] A. Doig, "Off-grid electricity for developing countries," IEE Review, vol. 45, Issue 1, pp 25–28, January 1999.

[3] L. Mateu and F. Moll, "Review of energy harvesting techniques and applications for microelectronics (Keynote Address)," in VLSI Circuits and Systems II, Sevilla, Spain, pp. 359–373, 2005.

[4] M. Arrawatia, M.S. Baghini, and G. Kumar, "RF energy harvesting system at 2.67 and 5.8GHz," IEEE Asia-Pacific Microwave Conference Proceedings, Yokohama, pp. 900–903, December 7–10, 2010.

[5] A. Boaventura, A. Collado, N.B. Carbalho, and A. Georgiadis, "Optimum behavior, wireless power transmission system design through behavioral models and efficient synthesis techniques," IEEE Microwave Magazine, vol. 14, no. 2, pp. 26–35, March 2013.

[6] T.T. Peter, T.A. Rahman, S.W. Cheung, R. Nilavalan, H.F. Abutarboush, and A. Vilches, "A novel transparent UWB antenna for photovoltaic solar panel integration and RF energy harvesting," IEEE Transactions on Antennas and Propagation, vol. 62, no. 4, pp. 1844–1853, April 2014.

[7] M. Arrawatia, M.S. Baghini, and G. Kumar, "RF energy harvesting from cell towers in 900MHz band," IEEE National Conference on Communications (NCC), Bangalore, pp. 1–5, January 28–30, 2011.

[8] D. Bouchouicha, F. Dupont, M. Latrach, and L. Ventura, "Ambient RF energy harvesting," International Conference on Renewable Energies and Power Quality, Spain, pp. 1–5, March 2010.

[9] J.A. Paradiso and T. Starner, "Energy scavenging for mobile and wireless electronics," IEEE Pervasive Computing, vol. 4, pp. 18–27, January–March 2005.

[10] K. Roth and J. Brodrick, "Energy harvesting for wireless sensors," ASHRAE Journal, May 2008.

[11] L. Mesica and A. Massaro, "New trends in energy harvaesting from Earth long- wave infrared emission," Advanced in Material Sciences and Engineering, vol. 2014, 2014.

[12] A. Arigliano, P. Caricato, A. Grieco, and E. Guerriero, "Producing, storing, using and selling renewable energy: the best mix for the small medium industry," Computers in Industry, vol. 65, no. 3, pp. 408–418, 2014.

[13] F. Manzano Agugliaro, A. Alcayde, F.G. Montoya, A. Zapata- Sierra, and C. Gil, "Scientific production of renewable energies worldwide: an overview," Renewable and Sustainable Energy Reviews, vol. 18, pp. 134–143, 2013.

[14] I. Kocakarin and K. Yegin, "Glass superstrate nanoantennas for infrared energy harvesting applications," International Journal of Antennas and Propagation, vol. 2013, Article ID 245960, 7 pp., 2013.

[15] R. Moghe, Y. Yang, and D.F. Divan, "A scoping study of electric and magnetic field energy harvesting for wireless sensor networks in power system applications," Energy Conversion Congress and Exposition, pp.3550–3557, 2009.

[16] Linear, 2014, Energy Harvesting Products, available at: http://www.linear.com/products/energyh arvesting

[17] Pavegen website, 2014, Technology Section, available at: http://www.pavegen.com/technology

[18] En Ocean website, 2014, Energy Harvesting Wireless Technology, available at: http://www.enocean.com /en/energy-harvesting-wireless/

[19] NikkoIA website, 2014, Applications, available at: http://www.nikkoia.com/en/biz-applications/security/

[20] Voltree Power website (2014), Bioenergy Harvester, available at: http://voltreepower.com/b ioHarvester.html

[21] A. Georgiadis, G. Andia, and A. Collado, "Rectenna design and optimization using reciprocity theory and harmonic balance analysis for electromagnetic (EM) energy harvesting," IEEE Antennas and Wireless Propagation Letters, vol.9, pp. 444–446, May 10, 2010.

[22] M. Zawadzki and J. Huang, "Integrated RF antenna and solar array for spacecraft application," in Proc. IEEE Int. Conf. Phased Array Syst. Technol., May 2000, pp. 239–242.

[23] Energy Harvesting Journal, 2010, An interview with Enocean by Raghu Das, available at: http://www.energyharvestingjournal.com/articles/an-interview-with-enocean-00002058.asp

[24] European Commission - Digital Agenda for Europe, 2014, Innovations in Energy Harvesting and Storage, Available at: http://ec.europa.eu/digital-agenda/futurium/en/content/innovations-energy-harvesting-and-storage

[25] Technology Strategy Board, 2011, Energy Harvesting: Watts Needed? Workshop, Royal Society, Carlton House Terrace London.

[26] A. Costanzo, F. Donzelli, D. Masotti, and V. Rizzoli, "Rigorous design of RF multi-resonator power harvesters," IEEE Proceedings of the Fourth European Conference on Antennas and Propagation, Barcelona, pp. 1–4, April 12–16, 2010.

[27] S.J. Orfanidis, "Electromagnetic waves and antennas," 2008, Rutgers University, Piscataway, New Jersey, USA, [Online], available at: http://www.ece.rutgers.edu/~orfanidi/ewa/ [Accessed April 2012]

[28] S. Rivière, A. Douyère, F. Alicalapa, and J.D. Lan Sun Luk, "Study of complete WPT system for WSN applications at low power level," Electronics Letters, Institution of Engineering and Technology, vol. 46, Issue 8, pp. 597–598, April 15, 2010.

[29] V. Rizzoli, D. Mascotti, N. Arbizzani, and A. Costanzo, "CAD procedure for predicting the energy received by wireless scavenging systems in the near-and far-field regions," IEEE Microwave Symposium Digest (MTT-S International), Bologna, pp.1, May 23–28, 2010.

[30] H. Jabbar, Y.S. Song, and T.T. Jeong, "RF energy harvesting system and circuits for charging of mobile devices," IEEE Transactions on Consumer Electronics, vol. 56, Issue 1, pp. 247–253, February 2010.

[31] M. Mi, M.H. Mickle, C. Capelli, and H. Swift, "RF energy harvesting with multiple antennas in the same space," IEEE Antennas and Propagation Magazine, vol. 47, no. 5, pp. 100–106, October 2005.

[32] T.S. Salter Jr., G. Metze, and N. Goldsman, "Improved RF power harvesting circuit design," International Semiconductor Research Symposium Proceedings, College Park, MD, USA, pp.1-2, December 12–14, 2007.

[33] D.G. Rowe, "Nokia developing phone that recharges itself without mains electricity," www.guardian.co.uk, Wed., June 10, 2009.

[34] W. Sun, N.P. Kherani, K.D. Hirschman, L.L. Gadeken, and P.M. Fauchet, "A three-dimensional porous silicon p-n diode for betavoltaics and photovoltaics,"Advanced Materials, 17, pp.1230–1233, 2005.

[35] V. Sakamuri and J. Frolik, "Design of a 2.4 GHz interrogator for a rectenna-based sensor system," IEEE 12th Annual Wireless and Microwave Technology Conference (WAMICON), pp.1–4, April 2011.

[36] J.W. Zhang, K.Y. See, and T. Svimonishvili, "Printed decoupled dual-antenna array on-package for small wirelessly powered battery-less device," IEEE Antennas and Wireless Propagation Letters, vol. 13, pp. 923–926, 2014.

[37] I.T. Nassar and T.M. Weller, "Development of novel 3-D cube antennas for compact wireless sensor nodes," IEEE Transactions on Antennas and Propagation, vol. 60, no. 2, pp. 1059–1066, February 2012.

[38] S.H. Nasab, M. Asefi, L. Albasha, N. Qaddoumi, "Investigation of RF signal energy harvesting," Active and Passive Electronic Components Journal (Hindawi Publishing Corporation), vol. 2010, Article ID 591640, pp.1–7, October 2010.

[39] T. Salter, K. Choi, M. Peckerar, G. Metze, and N. Goldsman, "RF energy scavenging system utilizing switched capacitor DC-DC converter," Electronics Letters (Institution of Engineering and Technology, Maryland, USA), vol. 45, Issue 7, pp. 374–376, March 26, 2009.

[40] J. Hautcoeur, L. Talbi, and K. Hettak, "Feasibility study of optically transparent CPW-fed monopole antenna at 60-GHz ISM bands," IEEE Transactions on Antennas and Propagation Magazine, vol. 61, pp. 1651–1657, 2013. T.W. Turpin and R. Baktur,

"Meshed patch antennas integrated on solar cells," IEEE Antennas and Wireless Propagation Letters, vol.8, pp. 693–696, 2009.

[41] Z. J. Wu, W.L. Biao, S.K. Yak, T.C. Ming, B.C. Chye, Y.K. Seng, and D.M. Anh, "Wireless energy harvesting using serially connected voltage doublers," Proceedings of the 2010 Asia-Pacific Microwave Conference, Yokohama, pp. 41–44, December 7–10, 2010.

[42] J. Ayers, K. Mayaram, and T.S. Fiez, "An ultralow-power receiver for wireless sensor networks," IEEE Journal of Solid-State Circuits, vol. 45, Issue. 9, pp. 1759–1769, August 23, 2010.

[43] P. Khoury, "A power-efficient radio frequency energy-harvesting circuit", Master thesis, Electrical Engineering Department, University of Ottawa, Ontario, Canada, January 2013.

[44] J.M. Ick and Y.B. Jung, "Novel energy harvesting antenna design using a parasitic radiator", Progress In Electromagnetics Research, vol. 142, pp. 545–557, 2013.

[45] N. Md. Din, C.K. Chakrabarty, A. Bin Ismail, K.K.A. Devi, and W.Y. Chen, "Design of RF energy harvesting system for energizing low power devices," Progress in Electromagnetics Research, vol. 132, pp. 49–69, 2012.

[46] A. Rahman, A. Alomainy, and Y. Hao, "Compact body-worn coplanar waveguide fed antenna for UWB body-centric wireless communications", European Conference on Antennas and Propagation, November 2007.

[47] Z.W. Sim, R. Shuttleworth, M.J. Alexander, and B.D. Grieve, "Compact patch antenna design for outdoor RF energy harvesting in wireless sensor networks," Progress In Electromagnetics Research, vol. 105, pp. 273–294, 2010.

[48] R.C. Hansen and R.E. Collin, Small Antenna Handbook, John Wiley and Sons Inc., IEEE Press, 2011.

[49] T. Szepesi and K. Shum (Analog Devices), "Cell phone power management requires small regulators with fast response," EE Times News and Analysis, February 2002. [Online] available at http://www.eetimes.com/electronics-news/4164128/Cell-phone-power-management-requires-small-regulators-with-fast-response [Retrieved April 2012].

[50] Rogers Corporation, "RT/duroid® 6006/6010LM High Frequency Laminates Data Sheet Rev 1.60000," Advanced Circuit Materials Division, Chandler, AZ. Publication: #92-105. Revised 03/2011. [Online], available at http://www.rogerscorp.com/documents/612/acm/RT-duroid-6006-6010-laminate-data-sheet, Retrieved June 2012.

[51] M. Arrawatia, M.S. Baghini, and G. Kumar, "RF energy harvesting system from cell towers in 900MHz band," Communications (NCC), 2011 National Conference, pp.1–5, January 28–30, 2011.

[52] J.P. Thomas, M.A. Qidwai, and J.C. Kellogg, "Energy scavenging for small-scale unmanned systems," Journal of Power Sources, vol. 159, pp. 1494–1509, 2006.

[53] W.C. Brown, "Status of the microwave power transmission components for the solar power satellite," IEEE Transactions on Microwave Theory and Techniques, vol. MTT-29, no. 12, pp.1319 –1327, 1981.

[54] M.A. Malek, S. Hakimi, S.K.A. Rahim, and A.K. Evizal, "Dual-band CPW fed transparent antenna for active RFID tags," IEEE Antennas and Wireless Propagation Letters, 2015.

[55] J.S. Hyok, Y.H. Tsung, D.F. Sievenpiper, P.H. Hui, J. Schaffner, and E. Yasan, "A method for improving the efficiency of transparent film antennas," IEEE Antennas and Wireless Propagation Letters, vol. 7, pp. 753–756, 2008.

[56] T. Paing, J. Shin, R. Zane, and Z. Popovic, "Resistor emulation approach to low-power RF energy harvesting," IEEE Transactions on Power Electronics, vol. 23. Issue 3, pp. 1494–1501, May 2008.

[57] D. Masotti, A.Constanzo, and S. Adam, "Design and realization of a wearable multi-frequency RF energy harvesting system," 5th European Conference on Antennas and Propagation (EUCAP) Proceedings, Rome, pp. 517–520, April 11–15, 2011.

[58] A.S. Weddell, G.V. Merrett, T.J. Kazmierski, and B.M. El-Hashimi, "Accurate supercapacitor modeling for energy harvesting Wireless Nodes," IEEE Transactions on Circuits and Systems-II: Express Briefs, vol. 58, no.12, pp. 911–915, December 2012.

[59] F. Raval and J. Makwana, "Optimization of resonance frequency of circular patch antennas at 5 GHz using practical swarm optimization", International Journal of Advances in Engineering and Technology, May 2011.

[60] A. Yu and X. Zhang, "A broadband patch antenna array for wireless LANs," IEEE Antennas and Propagation Society International Symposium, pp. 228–231, vol. 26–21, June 2002.

[61] M. Ali, G. Yang, and R. Dougal, "A new circularly polarized rectenna for wireless power transmission and data communication," IEEE Antennas and Wireless Propagation Letters, vol. 4, pp. 205–208, January 2005.

[62] K. Chung, Y. Nam, T. Yun, and J. Choi, "Reconfigurable microstrip patch antenna with switchable polarization," ETRI Journal, vol. 28, pp. 379–382, March 2006.

[63] H. Liu, S. Lin, and C. Yang, "Compact inverted-F antenna with meander shorting strip for laptop computer WLAN applications" IEEE Antenna and Wireless Propagation Letters, vol. 10, pp. 540–543, 2011.

[64] Z.W. Sim, R. Shuttleworth, and B. Grieve, "Investigation of PCB microstrip patch receiving antenna for outdoor rf energy harvesting in wireless sensor networks", 2009 IEEE Conference on Antennas and Propagation Proceedings, Loughborough, pp. 129–132, November 16-17, 2009.

[65] P. Borja and N. Romeu, "An iterative model for fractal antennas: application to the sierpinski gasket antenna," IEEE Transactions on Antennas and Propagation, vol. 48, no. 5, pp. 713–719, May 2000.

[66] S.B. Neetu and R.K. Bansal, "Design and Analysis of Fractal Antennas based on koch and sierpinski fractal geometries," International Journal of Advanced Research in Electrical, Electronics and Instrumentation Engineering, vol. 2, June 2013.

[67] T.Q.V. Hoang, A. Douyere, JL. Dubard, and JD. Lan Sun Lunk, "TLM design of a compact PIFA rectenna," 2011 International Conference on Electromagnetics in Advanced Applications (ICEAA), pp. 508–511, September 12–16, 2011.

[68] Y. Fujino, M. Fujita, N. Kaya, S. Kunimi, M. Ishii, N. Ogihata, N. Kusaka, and S. Ida, "A dual polarization microwave power transmission system for microwave propelled airship experiment," Proc. de ISAP'96, vol. 2, pp. 393–396, 1996.

[69] B. Strassner and K. Chang, "5.8-GHz circularly polarized rectifying antenna for wireless microwave power transmission," IEEE Transactions on Microwave Theory and Techniques, vol. 50, pp. 1870–1876, August 2002.

[70] C.K. Chin, Q. Xue, and C.H. Chan, "Design of a 5.8-GHz rectenna incorporating a new patch antenna," IEEE Antenna and Wireless Propagation Letters, vol. 4, pp. 175–178, 2005.

[71] G. Kumar and K.P. Ray, "Broadband microstrip antennas," Artech House, Inc., 2003.

[72] Jawad K. Ali, "A New Reduced Size Multiband Patch Antenna Structure Based on Minkowski prefractal Geometry," Journal of Engineering and Applied Sciences, vol. 2, no. 7, pp. 1120–1124, 2007.

[73] T.A. Milligan, "Modern antenna design," 2nd Edition, IEEE Press, 2005.

[74] S. Shrestha, S.K. Noh, and D.Y. Choi, "Comparative study of antenna designs for RF energy harvesting," 10 pp., 2013.

[75] S. Kim, "RF energy harvesting techniques for wirelessly powered devices," in Proceedings of the IEEE MTT-S International Microwave Workshop Series on Intelligent Radio for Future Personal Terminals (IMWS-IRFPT '11), Daejeon, Republic of Korea, 2011.

[76] R. Selvakumaran, W. Liu, B.H. Soong, L. Ming, and Y.L. Sum, "Design of low power rectenna for wireless power transfer," Tencon IEEE Region 10 Conference, Singapore, pp. 1–5, January 2009.

[77] A.M. Soliman, D.M. Elsheakh, E.A. Abdallah, and H.M. El-Hennawy, "Inspired metamaterial quad-band printed inverted-F (IFA) antenna for USB applications," The Applied Computational Electromagnetics Society (ACES) Journal, pp. 564–570, May, 2015.

[78] A.M. Soliman, D.N. Elsheakh, and E.A. Abdallah, "Low SAR multiband CPW fed PIFA with independent resonant frequency control for wireless communication applications," IET Microwaves, Antennas and Propagation, vol. 8, pp. 207–216, 2014.

[79] D. Elsheakh and A.M.E. Safwat, "Slow-wave quad-band printed inverted-F antenna (IFA)," IEEE Transactions on Antennas and Propagation, vol. 62, no. 8, pp. 4396–4401, 2014.

[80] A.M. Soliman, D.N. Elsheakh, E.A. Abdallah, and H. Elhenawy, "Reconfigurable independent multiband CPW-fed printed F-antenna for USB applications," Microwave and Optical Technology Letters, vol. 56, no.10, pp. 2237–2245, 2014.

[81] B.A. Munk, Frequency Selective Surfaces: Theory and Design, Wiley, New York, NY, 2000.

[82] A.M. Soliman, D. N. Elsheakh and Esmat A. Abdallah, Hadia Elhenawy, "Multi-Band Printed Metamaterial Inverted-F Antenna (IFA) for USB Applications", IEEE Antennas and Wireless Propagation Letters, vol. 15, pp. 297–300, 2015.

[83] D. Elsheakh, A. M. Soliman, and E. Abdallah, "Design of Planar Inverted F-Antenna over Uniplanar EBG Structure for Laptop MIMO Applications" IEEE international symposium on antenna and propagation AP-S, Memphis, Tennessee, 2014, USA.

[84] D. Elsheakh, A. M. Soliman, H. M. Elhennawy and E. Abdallah, "Compact Independent Tri-band Printed IFA loaded with Inspired Metamaterial for wireless Communication Applications", The 7th European Conference on Antennas and Propagation (EuCAP) 8-12 April in Gutenberg, Sweden, 2013.

[85] A.M. Soliman, D.N. Elsheakh, E.A. Abdallah, and H. Elhenawy, "Design of planarinverted F-antenna over uniplanar EBG structure for laptop MIMO applications," Microwave and Optical Technology Letter, vol. 57, pp. 277–285, February 2015.

[86] H. Laborat, "Microwave Power Transmission System Studies", vol. IV , Raytheon Company, Equipment Division, -7 - SUDBURY, MASS. 01776.

[87] Z. Zhang, A.W. Bargioni, S.W. Wu, S. Dhuey, S. Cabrini, and P. J. Schuck, "Manipulating nanoscale light fields with the asymmetric bowtie nano-colorsorter," vol. 12, pp. 4505–4509, 2009.

[88] R. Vogelgesang and A. Dmitriev, "Real-space imaging of nano-plasmonic resonances," Analyst 135, pp. 1175, 2010.

[89] T. Xu, Y.K. Wu, X. Luo, and L.J. Guo, "Plasmonic nano-resonators for higher solution colour filtering and spectral imaging," Nature Communications 1, vol. 59, 2010.

[90] J.J. Greffet, M. Laroche, and F. Marquier, "Impedance of a nano-antenna and a single quantum emitter," Physical Review Letters, vol. 105, 2010.

[91] W. C. Brown, "Status of the microwave power transmission components for the solar power satellite," IEEE Trans. Microw. Theory Tech., vol. 29, pp. 1319–1327, Dec. 1981.

[92] Y. K. Tan and S. K. Panda, "Energy harvesting from hybrid indoor ambient light and thermal energy sources for enhanced performance of wireless sensor nodes," IEEE Trans. Ind. Electron., vol. 58, no. 9, pp. 4424–4435, Sep. 2011.

[93] J. Colomer et al., "Novel autonomous low power VLSI system powered by ambient mechanical vibrations and solar cells for portable applications in a 0.13_ technology," in Proc. IEEE Power Electron. Specialists Conf., Jun. 17–21, 2007, pp. 2786–2791.

[94] K. Ko, A. Kumar, K.H. Fung, R. Ambekar, G.L. Liu, N.X. Fang, and K.C. Toussaint, Jr., "Nonlinear optical response from arrays of Au bowtie nanoantennas," Nano Letters, vol. 61, 2011.

[95] H. Matsumoto, "Research on solar power satellites and microwave power transmission in Japan," IEEE Microw. Mag., vol. 3, no. 4, pp. 36–45, Dec. 2002.

[96] A. Georgiadis and A. Collado, "Solar powered class-e active antenna oscillator for wireless power transmission," in Proc. IEEE Radio Wireless Symp., Jan. 20–23, 2013, pp. 40–42.

[97] C. Guclu, T.S. Luk, G.T.Wang, F. Capolino, "Radiative emission enhancement using nano-antennas made of hyperbolic metamaterial resonators," *Appl. Phys. Lett.* 2014, 105, 123101, doi:10.1063/1.4895816.

IntechOpen